FOCUSED ISSUE FEATURE

How Low Can They Go?

Ajay K. Poddar, Ulrich L. Rohde, and Anisha M. Apte

IMAGE LICENSED BY INGRAM PUBLISHING

Noise is associated with all the components of the oscillator circuit; however, the major contribution of the noise in an oscillator is from the active device, which introduces amplitude modulation (AM) and phase modulation (PM) noise [1]–[103]. The conventional wisdom is to ignore AM component of the noise because the gain limiting effects of the active device operating under saturation, allowing only little variation in the output amplitude due to the noise in comparison to PM noise component, which directly affects the frequency stability of the oscillator and creates noise sidebands. But in reality, many oscillator topologies create significant AM noise, therefore effective noise contribution is the combination of $1/f$ spectrum with the $1/f^2$ effect in all PM, makes the low-frequency noise much greater, and that's where the information in most modulated signals resides [1]–[3].

Ajay K. Poddar (akpoddar@synergymwave.com) and Ulrich L. Rohde (ulr@synergymwave.com) are with Synergy Microwave Corporation, New Jersey, USA and Technical University Munich (TUM), Germany. Ulrich L. Rohde is with Cottbus University, BTU Germany. Anisha M. Apte (anisha_apte@ieee.org) is with Synergy Microwave Corporation, New Jersey, USA.

Digital Object Identifier 10.1109/MMM.2013.2269859
Date of publication: 6 September 2013

1527-3342/13/$31.00©2013IEEE

Comments on Oscillator Noise Model

There are mainly two types of noise sources in bipolar oscillator circuit: broadband noise sources due to thermal and shot noise effects and the low-frequency noise source due to $1/f$ (flicker noise effects) characteristics. In field effect transistor (FET) oscillator, high-field diffusion noise is dominant and exhibits no shot noise.

The current flow in a transistor is not a continuous process but is made up of the diffusive flow of a large number of discrete carriers, and the motions of these carriers are random and explain the noise phenomenon up to certain degree, however there are many unknown. In conventional terms, the thermal fluctuation in the minority carrier flow and generation-recombination processes in the semiconductor device generates thermal noise, shot noise, partition noise, burst noise, and $1/f$ noise [4]. But in reality, this is not the case; the source of $1/f$ noise is still a subject of research, and physicists are still arguing about what causes it.

The phenomenon of PN generation in oscillators/voltage-controlled oscillators (VCOs) has been the main focus of important research efforts, and it is still an open issue despite significant gains in practical experience and modern CAD tools for design. In the design of VCOs, minimizing the PN is usually an important task and these objectives have been accomplished using empirical rules or numerical optimizations, and to this end, are often held as trade secrets by many manufacturers [5]–[12]. The ability to achieve optimum PN performance is paramount in most RF designs and the continued improvement of PN in oscillators is required for the efficient use of the frequency spectrum.

The degree to which an oscillator generates constant frequency throughout a specified period of time is defined as the frequency stability of the oscillator and the cause of the frequency instability is due to the presence of noise in the oscillator circuit that effectively modulates the signal, causing a change in frequency spectrum commonly known as PN. PN and timing jitter are both measures of uncertainty in the output of an oscillator. In conventional wisdom, PN defines the frequency domain uncertainty of an oscillator, whereas timing jitter is a measure of oscillator uncertainty in the time domain [13]–[33]. But in reality, PN and time jitter correlate each other and tells same thing. The main distinction is just that "jitter" is applied primarily to digital sources. The equation for ideal sinusoidal oscillator in time domain is given by

$$V_{\text{out}}(t) = A\cos(2\pi f_0 t + \varphi), \tag{1}$$

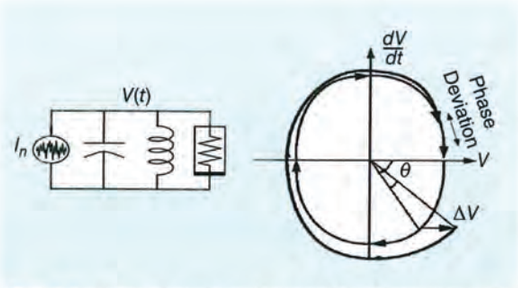

Figure 1. *A typical limit cycle of an ideal LC oscillator (the current noise perturbs the oscillator's voltage by ΔV and the perturbed signal restores its stable amplitude whereas its phase is free to drift, causing strong random phase variations).*

where A, f_0, and φ are the amplitude, frequency, and fixed phase of the oscillator.

The output voltage of a real oscillator in time domain is given by

$$\begin{aligned} V_{\text{out}}(t) &= A(t)\cos[\omega_0 t + \varphi(t)] \\ &= [A + \alpha(t)]\cos[2\pi f_0 t + \varphi(t)] \end{aligned} \tag{2}$$

where $A(t)$, $\varphi(t)$, and f_0 are the time variable amplitude fluctuation, frequency and time variable phase fluctuation, frequency of the oscillator respectively.

As a consequence of the fluctuations, the spectrum of a practical oscillator is broadened. In practice, amplitude noise (AM noise) is smaller than phase-noise (PN) due to the amplitude-restoring mechanism in LC oscillators, this is illustrated by the limit cycle of an ideal LC oscillator as shown in Figure 1 [34]–[37]. The current noise perturbs the signal and causes its phasor to deviate from the stable trajectory, producing both amplitude and PN. The amplitude deviation is resisted by the stable limit cycle, whereas the phase is free to drift. Therefore, oscillators almost exclusively generate PN near the carrier. Figure 2(a), (b), and (c) illustrates the frequency spectrum and typical PN plot of oscillators, and the frequency fluctuation corresponding to jitter in the time domain, which is random perturbation of the zero crossing of a periodic signal. From (1) and (2), the fluctuation introduced by $A(t)$ and $\varphi(t)$ are functions of time and lead to sidebands around the center frequency f_0. The single sideband (SSB) PN $L(f)$ is usually expressed in the frequency domain and described in units of dBc/Hz, representing the noise power relative to the carrier contained in a 1 Hz bandwidth centered at a certain frequency offset from the carrier.

In the order of increasing complexity, noise models are grouped into one of the three categories as: linear time invariant (LTIV), linear time variant (LTV), and nonlinear time variant (NLTV). Leeson's model [1] is based on LTIV properties of the oscillator, such as resonator Q, feedback gain, output power, and noise figure; a second model is proposed by Lee and Hajimiri [35],

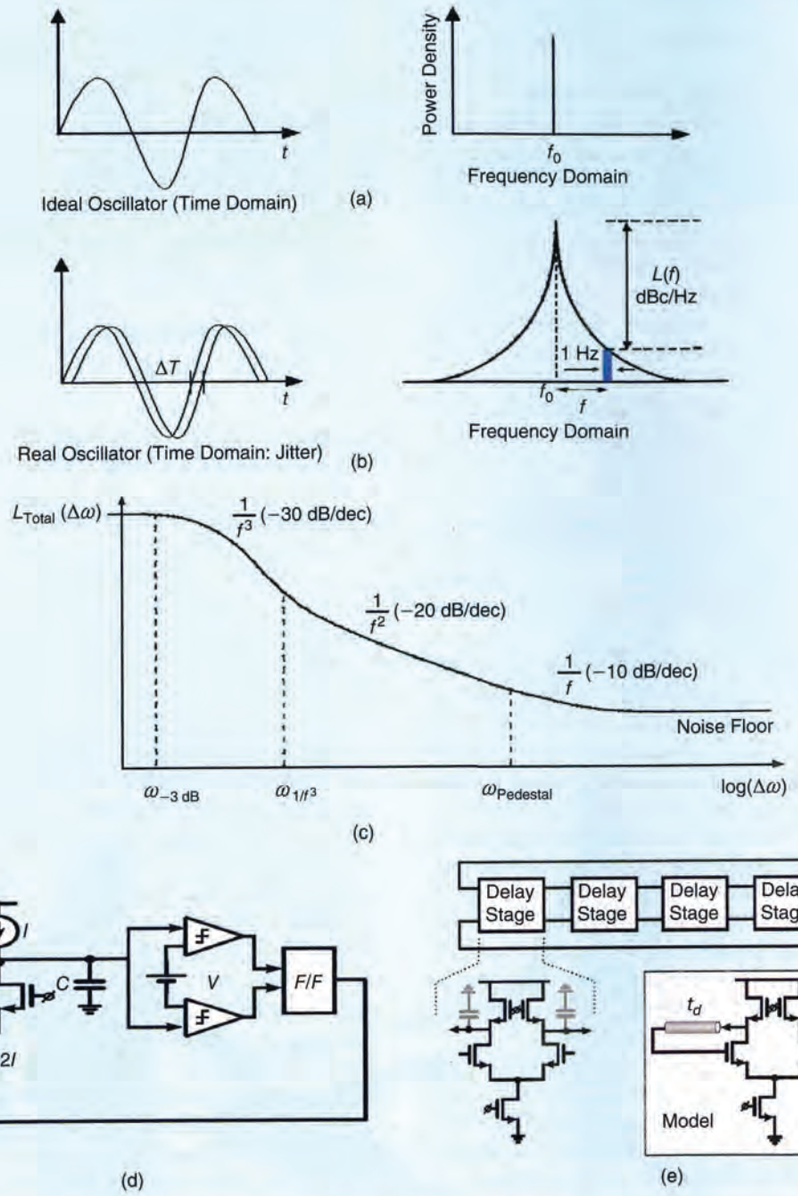

Figure 2. *(a) A frequency spectrum of ideal and real oscillators, (b) jitter in time domain relates to phase noise in the frequency domain, (c) a typical phase noise plot of real oscillator, (d) a typical simplified relaxation oscillator circuit [69], and (e) a typical simplified ring oscillator circuit using a CMOS device and equivalent model to calculate the additive noise transfer function [69].*

based on time-varying properties of the oscillator RF current waveform (LTV); and a third is proposed by Kaertner and Demir using a perturbation model based on numerical techniques (NLTV) [38], [39], [46], and [47].

Nallatamby et al. [6] revisited the Lesson's noise model, providing a detailed and enlightening analysis, demonstrating its applicability to several oscillator circuits. The theories proposed by Hajimiri and Lee and from Kaertner and Demir are based on time-domain approaches for harmonic oscillator circuits (like LC resonator). The approach from Hajimiri and Lee can be seen as a particular case of the theory of Kaertner and Demir, as it can be shown in the analytical comparison between time and frequency-domain techniques for PN analysis, carried out by Suárez et al. [7]. The impulse sensitivity function (ISF) proposed by Hajimiri and Lee can be employed to optimize the PN performances of a given oscillator and ISF can be obtained from harmonic balance (HB) as shown by Ver Hoeye et al. [8]. More insight and improvements of PN analysis that can be implemented using commercially available HB tools can be found in the paper of Sancho et al. [9].

It is important to distinguish noise dynamics in resonator-based oscillators (harmonic oscillators) with a sharply contrasting oscillator type, time/waveform based oscillator (like relaxation, ring, and multivibrator) [69]. Generically this comprises a single reactance, almost always a capacitor, a regenerative memory element such as a flip-flop or Schmitt trigger, and a means of charging and discharging the capacitor [Figure 2(d)].

Typically, harmonic oscillators can be characterized by equivalence to two energy storage reactive elements (inductor and capacitor), exchanging electrical and magnetic energy at resonance in order to give a periodic output signal. The actual LC resonant element can be high quality factor surface acoustic wave (SAW) resonator or quartz crystal resonator or dielectric resonator or printed transmission line or lumped inductor-capacitor resonator. The time/waveform based RC oscillator circuits (like relaxation, ring, multivibrator) use one energy storage reactive element typically "capacitor") for determining oscillation frequency. The single reactance is not frequency selective like the resonator, and the regenerative element makes this into a discrete-time feedback loop. The basis of noise dynamics is fluctuation-dissipation theorem of thermodynamics in conjunction with probability viewpoints using the concept of Brownian motion (Wiener process), which dictates a lower limit for PN in *RC* oscillators. Specifically, the PN due to the distinct characteristics of threshold crossing in RC oscillators can be expressed as functions of temperature, power dissipation, frequency of oscillation and the offset frequency. In the family of inductor less oscillator, ring oscillator is most useful for current and later generation communication systems. As shown in Figure 2(e), the ring oscillator derives its frequency from the cumulative delay in the stages making up the ring. It follows by symmetry that if all the stages are identical, then as the sine wave traverses each stage of the ring its amplitude remains unchanged, and it experiences a phase lag of 45° [69]. For simplification in analysis, assume that only one of the delay stages in the ring is noisy, and the others are noiseless. Then for frequencies around f_c, the ring oscillator may be modeled as a single noisy differential pair with negative feedback from the output to the input via an ideal delay line, t_d [Figure 2(e)]. The unity gain delay line models the other three noiseless stages because its gain is one (specifically at the oscillation frequency), and we lump into it the delay of the entire ring, i.e. $t_d = 1/(2f_c)$.

The current flow in a transistor is not a continuous process but is made up of the diffusive flow of a large number of discrete carriers.

To have a better insight of the noise effects in the oscillator design, it is necessary to understand oscillator topologies how the noise arises in active (transistors) and passive devices. The designer has very limited control over the noise sources in a transistor, only being able to control the device selection and the operating bias point. However, using knowledge about how noise affects oscillator waveforms, the designer is able to substantially improve PN performance of the oscillator circuits by the optimization of the key parameters (large signal noise factor, output waveform symmetry, circuit topology, drive-level, and noise filtering techniques) [4]–[11].

Leeson's Phase Noise Model (LTI)

PN is usually characterized in terms of the signal sideband noise spectral density. It has units of decibels below the carrier per hertz (dBc/Hz) and is defined as

$$L_{\text{total}}\{\Delta\omega\} = 10 \cdot \log\left[\frac{P_{\text{sideband}}(\omega_0 + \Delta\omega, 1\,Hz)}{P_{\text{carrier}}}\right],$$

where $P_{\text{sideband}}(\omega_0 + \Delta\omega, 1\,Hz)$ represents the signal sideband power at a frequency offset of $\Delta\omega$ from the carrier with a measurement bandwidth of 1 Hz. Leeson's PN equation is given by [1]

$$\pounds(f_m) = 10\log\left\{\left[1 + \frac{f_0^2}{(2f_mQ_L)^2(1-\frac{Q_L}{Q_0})^2}\right]\left(1+\frac{f_c}{f_m}\right)\frac{FkT}{2P_o}\right\}, \quad (3)$$

where $\pounds(f_m)$ = ratio of sideband power in a 1 Hz bandwidth at f_m to total power in dB, f_m = frequency offset from the carrier, f_0 = center frequency, f_c = flicker frequency, Q_L = loaded Q of the tuned circuit, Q_0 = unloaded Q of the tuned circuit, F = noise factor, kT = 4.1×10^{-21} at 300 K (room temperature), and P_o = average power at oscillator output.

It is important to understand that the Leeson model is based on LTIV characteristics and is the best case since it assumes the tuned circuit filters out all of the harmonics. Assuming the PN as a small perturbation, Leeson linearizes the oscillator circuit around the steady-state point in order to obtain a closed-form formula for PN. In all practical cases, it is hard to predict what the operating Q and noise figure will be. The predictive power of the Leeson model is limited due to the following which is not known prior to measurement: the output power, the noise figure under large signal conditions, and the loaded Q. This classic paper [1] is good design guide with the basic understanding

Typically, harmonic oscillators can be characterized by equivalence to two energy storage reactive elements, exchanging electrical and magnetic energy at resonance in order to give a periodic output signal.

that the "noise factor" as shown in (3) is not what we normally think of, but a measure of the upconverted $1/f$ noise. Since Leeson's model does not try to account for this, it cannot possibly provide useful noise predictions. The drawback of this approach is the fact that the up-conversion of the low frequency flicker noise components to around carrier PN, which is a necessary input to the equation; the RF output power, the loaded Q, and the noise factor of the amplifier under large signal condition, are not known. In addition to this (3) predicts an infinite PN power as $f \to 0$.

Rohde combined the Leeson PN (3) with the tuning diode contribution, that allows us to calculate the oscillator PN as [4]

$$L(f_m)=10\log\left\{\left[1+\frac{f_0^2}{(2f_mQ_L)^2}\right]\left(1+\frac{f_c}{f_m}\right)\frac{FkT}{2P_{sav}}+\frac{2kTRK_0^2}{f_m^2}\right\}, \quad (4)$$

where $L(f_m)$ = ratio of sideband power in a 1 Hz bandwidth at f_m to total power in dB, f_m = frequency offset, f_0 = center frequency, f_c = flicker frequency, Q_L = loaded Q of the tuned circuit, F = noise factor, $kT = 4.1\times10^{-21}$ at 300 K_0 (room temperature), P_{sav} = average power at oscillator output, R = equivalent noise resistance of tuning diode (typically 50 Ω – 10 kΩ), and K_o = oscillator voltage gain.

The limitation of this equation is that the loaded Q in most cases has to be estimated and the same applies to the noise factor. The microwave harmonic-balance simulator, which is based on the noise modulation theory (published by Rizzoli), automatically calculates the loaded Q and the resulting noise figure as well as the output power [40]. When adding an isolating amplifier, the noise of an LC oscillator system is determined by

$$\begin{aligned}S_\phi(f_m) = {} & [a_RF_0^4 + a_E(F_0/(2Q_L))^2]/f_m^3 \\ & + [(2GFkT/P_0)(F_0/(2Q_L))^2]/f_m^2 \\ & + (2a_RQ_LF_0^3)/f_m^2 \\ & + a_E/f_m + 2GFkT/P_0, \end{aligned} \quad (5)$$

where, G = compressed power gain of the loop amplifier, F = noise factor of the loop amplifier, k = Boltzmann's constant, T = temperature in Kelvin, P_0 = carrier power level (in watts) at the output of the loop amplifier, F_0 = carrier frequency in hertz, f_m = carrier offset frequency in hertz, $Q_L = (\pi F_0\tau_g)$ = loaded Q of the resonator in the feedback loop, and a_R and a_E flicker noise constants for the resonator and loop amplifier.

There is a misunderstanding that the loaded Q is always infinite in steady-state condition and leads to 0 Hz noise bandwidth for the negative resistance oscillator circuit. And, if this is the case then his oscillator would take infinite time to build the output transient waveform and reach at the stable state condition. In reality, there is net resistance at turn-on, and the start-up transient depends on the behavior of the nonlinearity associated with the oscillator circuits and the slope parameter of resonator establishes the noise spectrum [42].

Although Leeson's PN model provides a valuable insight into the oscillator design from engineering perspectives, it cannot explain some of the important PN phenomena. This is due to simplifying assumptions made about the linearity and time-invariant behavior of the system. When comparing the measured results of oscillators with the assumptions made in Leeson's equation, one frequently obtains a de facto noise figure in the vicinity of 20–30 dB and an operating Q that is different than the assumed loaded Q, therefore must be determined from measurement; diminishing the predictive power of the Leeson's PN.

Leeson's model observes the asymptotic behavior of PN at close-to carrier offsets, asserting that PN goes to infinity with $1/f^3$ rate. This is obviously wrong as it implies an infinite output power for oscillator. For noisy oscillators it could also suggest that $L(f) > 0$ dBc/Hz, this singularity arises from linearity assumption for oscillator operation around steady-state point. In fact, the linear model breaks down at close-to-carrier frequencies where the PN power is strong [39]. Considering a nonlinear model for the oscillator in absence of flicker noise, these singularities can be resolved by expressing the PN in the form of a Lorentzian function [42]

$$L(\Delta f_m) \propto \frac{a^2}{a^2+(\Delta f_m)^2}, \quad (6)$$

where a is a fitting parameter.

Although (6) models the spectrum and avoids any singularity at $\Delta f_m = 0$ while maintaining the same asymptotic behavior as illustrated in Figure 3; this is an after-the-fact approach, not a predictive one. From (6), the total power of PN from minus infinity to plus infinity is one, this means that PN doesn't change the total power of the oscillator; it merely broadens its spectral peak. Attempting to match the Leeson calculated curve "A" (Figure 3) considering (3), the measured curve requires totally different values than those assumed due to upconversion and down-conversion of noise components from harmonically related frequencies to around carrier frequency as depicted in Figure 4 [39].

Particularly, the effect of the low-frequency flicker noise components on close-in PN is not well characterized in Leeson's model. The model asserts that the PN $1/f^3$ corner frequency is exactly equal to the amplifier's flicker-noise corner frequency, ωc. However, measurements frequently show no such equality. This is because Leeson models the oscillator as a time-invariant system, whereas oscillators are in general cyclostationary (A cyclostationary process is a signal having statistical properties that vary cyclically with time) time-varying systems due to the presence of the periodic large-signal oscillation. This issue has been addressed by several authors. Hajimiri has shown that the oscillator's PN $1/f^3$ corner frequency can be significantly lower than the device's flicker corner frequency; provided that the oscillation signals at the output of the oscillator circuits is odd-symmetric [36].

The basic concept of the Leeson equation, however, is correct and gives a quick evaluation of the PN performance for oscillator circuits and also basic trend for the minimization of noise if following unknown terms are assumed and inserted properly, the computed results will agree within a reasonable degree of the accuracy. The information that is not known prior to measurement is:

a) the output power
b) the noise figure under large-signal conditions
c) the loaded (operational) noise figure
d) flicker up conversion dynamics
e) singularity at close to carrier.

In conclusion, Leeson's model assumes linear approach but oscillators are inherently nonlinear, it is expected that such a linear PN model would predict the PN of an oscillator with a significant error.

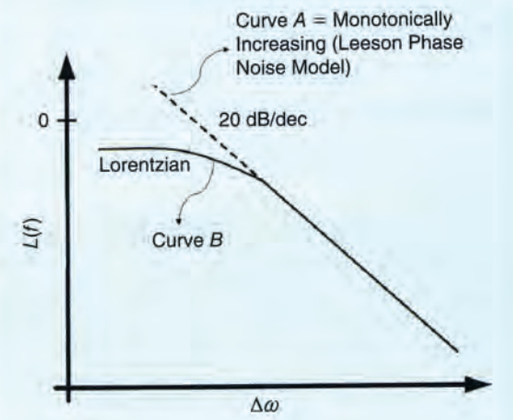

Figure 3. *Close-in PN behavior due to white noise sources. Leeson's model predicts that PN monotonically increases by approaching the carrier whereas in reality it takes the form of a Lorentzian shape [42].*

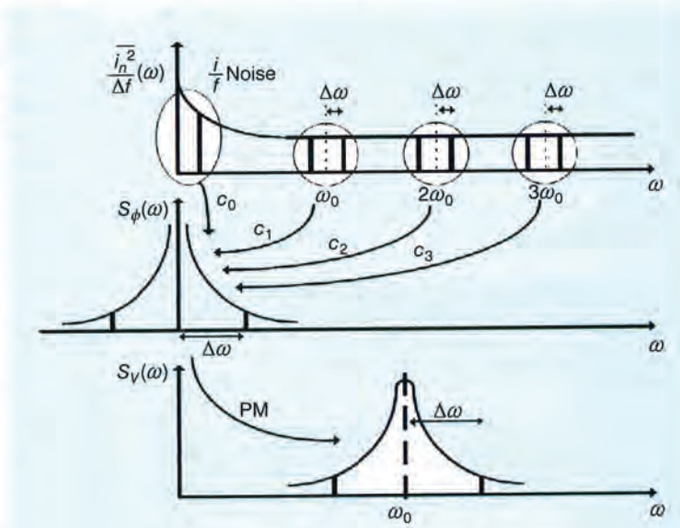

Figure 4. *The conversion process from noise [$Sn(\omega)$] to PN [$L(\omega)$]. Noise components from harmonically-related frequencies are up/down-converted to around carrier PN, and Leeson's model fails to address this phenomenon [36].*

Lee and Hajimiri's Noise Model (LTV)

To overcome the limitation of LTIV PN model (Leeson's PN model), Lee and Hajimiri proposed an LTV PN model to predict the noise properties of the oscillator output waveform [36], [43]–[45]. There were many LTV models around and before Lee and Hajimiri explaining the PN dynamics of autonomous circuits (oscillators) for a given nonlinearity associated with the circuits in large signal conditions. Lee and Hajimiri's noise model is based on the LTV properties of the oscillator current waveform, and the PN analysis is given based on the effect of noise impulse on a periodic signal. Figure 5 shows the noise signal in response of the injected impulse current at two different times, peak and zero crossing. As illustrated in Figure 5, if an impulse is injected into the tuned circuit at the peak of the signal, it will cause maximum AM and no PM whereas; if an impulse is injected at the zero crossing of the signal, there will be no AM but maximum PM. If noise impulses are injected between zero crossing and the peak, there will be components of both phase and AM. Variations in amplitude are generally ignored because they are limited by the gain control mechanism of the oscillator. Therefore, according to this theory, to obtain the minimal PN, special techniques have to be adopted so that any noise impulse should coincide in time with the peaks of the output voltage signal rather than at the zero crossing or in between of zero-crossing and peak.

It is important to understand that the Leeson model is based on LTIV characteristics and is the best case since it assumes the tuned circuit filters out all of the harmonics.

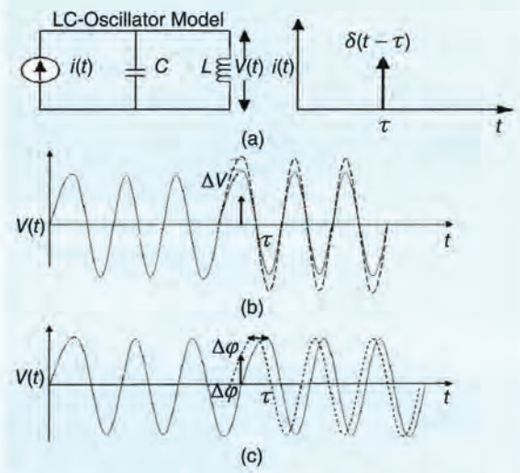

Figure 5. *(a) The LC oscillator excited by current pulse, (b) the impulse injected at the peak of the oscillation signal, and (c) the impulse injected at zero crossing of the oscillation signal.*

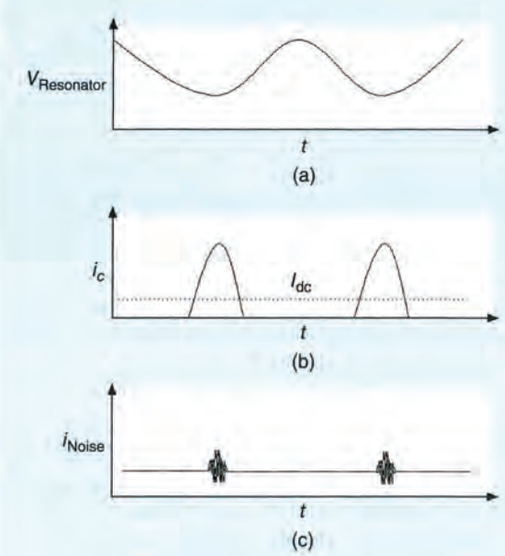

Figure 6. *(a) A voltage across resonator, (b) an oscillator output RF current, and (c) a noise current.*

Lee and Hajimiri introduced an ISF based on injected impulse, which is different for each topology of the oscillator. It has its largest value when the most PM occurs and has the smallest value when only AM occurs. This model is a kind of impulse response function that defines the PN versus device noise transfer function, in a manner similar to an impulse-response function in a linear circuit.

The calculation of the ISF is tedious and depends upon the topology of the oscillator. Based on this theory, PN equation is expressed as [36]

$$\pounds(f_m) = \begin{cases} 10\log\left[\dfrac{C_0^2}{q_{\max}^2} * \dfrac{i_n^2/\Delta f}{8f_m^2} * \dfrac{\omega_{1/f}}{f_m}\right] \dfrac{1}{f^3} \rightarrow \text{region} \\ 10\log\left[10\log\left[\dfrac{\Gamma_{\text{rms}}^2}{q_{\max}^2} * \dfrac{i_n^2/\Delta f}{4f_m^2}\right]\right] \dfrac{1}{f^2} \rightarrow \text{region} \end{cases}, \tag{7}$$

where $i_n^2/\Delta f$ = noise power spectral density, Δf = noise bandwidth, $\Gamma_{\text{rms}}^2 = 1/\pi \int_0^{2\pi} |\Gamma(x)|^2 dx = \sum_{n=0}^{\infty} C_n^2$ = root mean square (RMS) value of $\Gamma(x)$, $\Gamma(x) = C_0/2 + \sum_{n=1}^{\infty} C_n \cos(nx + \theta_n)$ = ISF, C_n = Fourier series coefficient, C_0 = 0th order of the ISF (Fourier series coefficient), θ_n = phase of the nth harmonic, f_m = offset frequency from the carrier, $\omega_{1/f}$ = flicker corner frequency of the device, and $q_{\max}$ = maximum charge stored across the capacitor in the resonator.

At first glance it appears that LTV model overcomes the shortcomings of LTIV model presented by Leeson. Careful inspection of Lee and Hajimiri LTV model revels that there are difficulties with its application to PN prediction. This follows since, apart from the ISF, the expression for the PN does not directly describe the effect of circuit parameters e.g. capacitance, inductances, resistance, transistor parameters, etc.). In order to obtain a quantitative PN solution for a circuit, the ISF has to be calculated by computer simulation on the oscillator circuit. Since analytical solutions for the ISF in terms of circuit parameters are mostly nonexistent, it can only be done numerically. Consequently, insight into how the physics of the circuit (the circuit parameters) can be manipulated to yield improved PN performance is lost.

Equation (7) is a generalization of Leeson's model if it is evaluated at the hand of underlying assumptions (shown in Figures 3 and 4) but it is a step closer to numerical computer simulation at the cost of analytical insight bound to physical parameters. While Leeson's model retained the loaded quality factor of the resonator (a physical parameter), the Lee and Hajimiri model does away with as many of the physical circuit parameters as possible (unifying the effect of such parameter into a single ISF). Various other conclusions are drawn that amount to manipulation of the ISF, but such conclusions are removed from what can be implemented through oscillator circuit design. Nevertheless LTV model does yield some insights that Leeson's model lack. First it reveals that if the active element in an oscillator were able to instantaneously restore the energy transferred to the resonator at precisely the right moment in the oscillation cycle, then it would in principle limit the PN to a minimum, which is validated by the examination of the Colpitts oscillator circuit [36]. Second, PN can be reduced by increasing the maximum charge displacement $q_{\max}$ in (7); this can in some case be physically accomplished by increasing the output power level of the oscillation signal-although this insight is more specific as it is something already known from LTIV based Leeson's model. Third, any PN present around integer multiples of the oscillation frequency is frequency translated to appear as PN sidebands around the oscillation signal. In conclusion, LTI-based noise model gives good results once all the data is known, but does not lead to exact design rules. Equation (7), using LTV theory though providing a good tool for explaining the PN spectrum in oscillators especially the $1/f^3$ region, suffers from a number of shortcomings:

a) It assumes oscillators are inherently LTV but does not give a concrete reason for this.
b) It is based on the parameter ISF, which is very difficult to determine.
c) It does not provide insight into the factors affecting performance in oscillator design.

The noise analysis based on signal drive level and the conduction angle of the time-varying properties of the oscillator current waveform can overcome partly the drawback associated with Lee and Hajimiri's noise model. The signal drive voltage produces an output current consisting of a series of current pulses, its shape and conduction angle depends upon the strength of the signal drive level. Figure 6(a), (b), and (c) shows the typical noise current i_{noise} relative to the RF current i_c for a LC-Colpitts oscillator in presence of resonator signal voltage $v_{\text{resonator}}$.

The natural operation of the oscillator will cause the current pulses to be centered on the negative peaks of the resonator voltages and the associated noise components depend on the conduction angle (width of the RF current pulse). From Rohde's noise model, the conduction angle $\varphi(\varphi \propto (1/C_2))$ is inversely proportional to the feedback capacitor C_2 and directly proportional to the drive-level $x(x \propto C_2)$. The following example given in the Figure 7 illustrates the circuit diagram of the 100-MHz LC Colpitts oscillator for giving insight into the relationship between the drive level, the current pulse, and the PN. As shown in Figure 8, the majority of noise current exists only during collector current pulses and

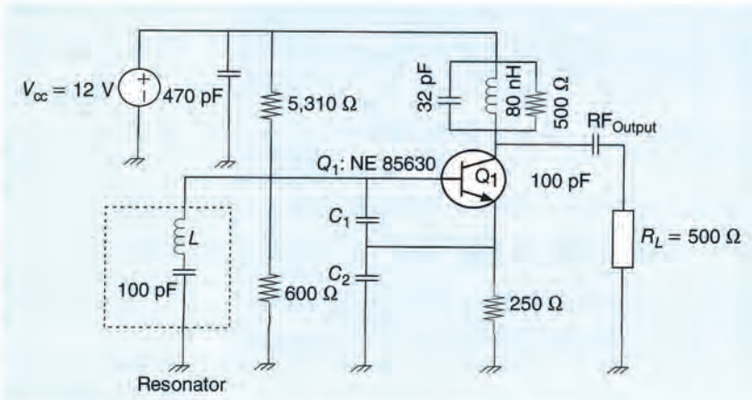

Figure 7. *A schematic of a typical 100-MHz LC colpitts oscillator.*

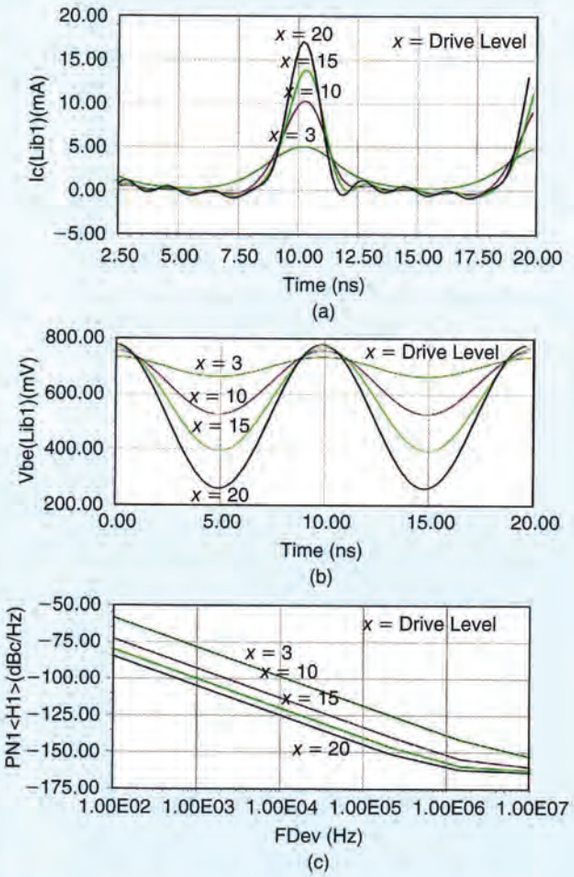

Figure 8. *(a) An RF current as a function of the normalized drive level x for the circuit in Figure (7), (b) an RF voltage V_{be} across the base emitter as a function of the normalized drive level x, and (c) a PN as a function of the normalized drive level x for the circuit in Figure (7).*

TABLE 1. Drive level for different values of C_2 for a 100-MHz oscillator.

$x=\frac{qV_{base}}{kT}$	C_1	C_2	L	Phase Noise at 10-KHz Offset	Frequency
3	500 pF	50 pF	80 nH	−98 dBc/Hz	100 MHz
10	500 pF	100 pF	55 nH	−113 dBc/Hz	100 MHz
15	500 pF	150 pF	47 nH	−125 dBc/Hz	100 MHz
20	500 pF	200 pF	42 nH	−125 dBc/Hz	100 MHz

the oscillator output current will be negligible or zero during the time between output current pulses, and therefore, aside from thermal noise, the noise sources, which depend on current such as shot, partition, and $1/f$, exist only during the conducting angle of output current pulses. If the signal drive level is increased, the oscillator output current pulse will be narrower, and consequently, noise pulse during conduction angle also becomes narrowed, and thereby, has less PM noise contribution than the wider pulse. Table 1 shows the drive level for different values of C_2 for a 100-MHz oscillator.

The collector current of the circuit shown in the Figure 7 plotted in Figure 8(a) using CAD simulator (Ansys: Ansoft Designer 8.1) becomes narrower as the drive level x increases, and the corresponding base voltage base V_{base} swing increases as illustrated in Figure 8(b). The improvement in the PN performance with respect to the drive level is shown in Figure 8(c), and it is limited by the strong harmonic content due to the large signal drive level. Introducing the signal drive level concept in conjunction with oscillator output current conduction angle, (3) can be expressed as [4, pp. 180]

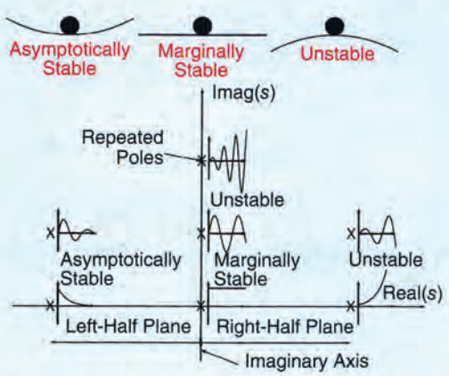

Figure 9. *The stability plane for asymptotically stable, marginally stable, and unstable condition.*

$$\pounds(\omega) = 10\mathrm{Log}\left\{\left[\left[4kTR + \left[\frac{4qI_c g_m^2 + \frac{4K_f I_b^{AF}}{\omega} g_m^2}{\omega_0^2 C_1^2 (\omega_0^2 (\beta^+)^2 C_2^2 + g_m^2 \frac{C_2^2}{C_1^2})}\right]\right] \times \left[\frac{\omega_0^2}{4\omega^2 V_{cc}^2}\right]\left[\frac{Q_O^2}{Q_L^2} + \frac{[C_1 + C_2]^2}{C_1^2 C_2^2 \omega_0^4 L^2 Q_L^2}\right]\right\}, \quad (8)$$

where

$$\beta^+ = \left[\frac{Y_{21}^+}{Y_{11}^+}\right]\left[\frac{C_1}{C_2}\right]^p;\ g_m = [Y_{21}^+]\left[\frac{C_1}{C_2}\right]^q.$$

Values of p and q depend upon the drive level Y_{21}^+, Y_{11}^+ = large signal $[Y]$ parameter of the active device, K_f = flicker noise coefficient, AF = flicker noise exponent, $\pounds(\omega)$ = ratio of sideband power in a 1 Hz BW at ω to total power in dB, ω = frequency offset from the carrier, ω_0 = center frequency, Q_L = loaded Q of the tuned circuit, Q_O = unloaded Q of the tuned circuit, $kT = 4.1 \times 10^{-21}$ at 300 K (room temperature), R = equivalent loss resistance of the tuned resonator circuit, I_c = RF collector current, I_b = RF base current, V_{cc} = RF collector voltage, and C_1, C_2 = feedback capacitor as shown in Figure 7.

Equation (8) gives clear insight and apriori estimation of the PN in terms of the operating condition and circuit parameters (validation examples and numerical results are described in [4, pp. 181–199]). However, all three noise models discuss and point out about the free-running oscillator and do not explain the PN improvement characteristics in the mutually coupled oscillator systems.

Kaertner, Demir, Ngoya's Noise Model (NTV)

Even though the LTV method is able to explain how the device noise around the oscillator's harmonics affects the PN, it is a matter of fact that the oscillator behavior is nonlinear by nature. So it can be expected that the results obtained from LTV noise model will not take into account, the associated nonlinearity in the oscillator circuits, hence cannot offer unified solution. For simplification in analysis, some approximations employed in the LTV method, turn out to be false assumption [48] even though it provides design flow for noise dynamics.

To overcome the limitation of LTV noise model, there have been several attempts to analyze the PN using NLTV techniques, perhaps the most acknowledged of these is presented by Kaertner and Demir in [38], [39], [46], and [47]. Kaertner and Demir pointed out the flaws of LTIV and LTV models that both the total integrated power and the noise power density at the carrier are infinite-a physical impossibility. To overcome these discrepancies, NLTV PN model was proposed from the fundamental differential equation description for a general oscillator by taking noise perturbation signals into account [39]. The proposed NLTV PN model is based on orbital asymptotic stability theory using white and modulated-white noise sources with power spectrum

falling $1/f^k$ for any $k \varepsilon N$, it is proved that such white and modulated-white noise sources led to a phase deviation, $\phi(t)$, which is characterized as a stochastic process with characteristic function, $F(\omega,t)$, described by a mean, $\mu(t)$, and a variance, $\sigma(t)$. Stability theory addresses the following questions: will a nearby orbit indefinitely stay close to a given orbit? Will it converge to the given orbit? In the former case, the orbit is called stable and in the latter case, asymptotically stable, or attracting. Figure 9 illustrates the stability planes for asymptotically stable, marginally stable, and unstable conditions.

For such white noise and modulated white noise sources, the PN power spectrum is analytically derived for angular frequency ω_0 of carrier signal as

$$S(\omega) = \sum_{k=-\infty}^{\infty} X_k X_k^* \frac{4\omega_0^2 k^2 p}{\omega_0 k^4 p^2 + 4(\omega + k\omega_0)^2}, \quad (9)$$

where X_k is Fourier coefficient of the asymptotically (as shown in Figure 9) orbitally stable periodic solution. This implies that n-dimensional stable limit cycle solution based on standard nonlinear analysis technique of linearizing around a nonlinear stable limit cycle solution, which means that $x_s(t)$ is simply the unperturbed oscillation signal) to the oscillation $x_s(t)$, as

$$x_s(t) = \sum_{k=-\infty}^{\infty} X_k e^{jk\omega_0 t} \quad (10)$$

$p = d/dt\,[\sigma^2(t)]$, which physically translates to the rate of change of the squared variance, σ to the Gaussian solution of the characteristic function, $F(\omega,t)$, of the phase deviation $\phi(t)$.

Equation (9) is so general that it does not even need to be an electrical system and valid for any physically realizable system (electrical, mechanical, biological, etc.) that exhibits stable oscillatory behavior. The NLTV PN model proposed by Kaertner and Demir using differential equations for describing the frequency and amplitude response of oscillators through perturbation techniques is unequalled in its generality, accuracy and efficient computational complexity, but the physics of the circuit is completely lost by a pure statistical characterization of the system. The solution of (9) is derived by computer but poorly suited to analytical computation by hand on paper (it is just like anything else that is useful, correct, and accurate in the world of nonlinearity).

To overcome the limitation of LTIV PN model, Lee and Hajimiri proposed an LTV PN model to predict the noise properties of the oscillator output waveform.

The initial guess of (9) is the $1/f^2$ PN reduction with frequency and so qualitatively reveals nothing more than what can be learned from linear PN models.

The noise model is based on differential equations describing the amplitude and phase deviations of the oscillator in terms of Taylor series expansions, assuming that the underlying device noise can be completely described stochastically. The stochastic differential equations so obtained are solved to obtain the final expression of PN. Since flicker noise is difficult to characterize in time domain, Kaertner and Demir obtain approximate series solutions. The time domain PN algorithm for (9) becomes numerically unstable when the concerned oscillator employs a high Q resonator (crystal resonator, $Q \cong 10^6$). Similarly, the frequency domain PN algorithm for (9) depends on the numerical method of HB using CAD simulator (AWR, Agilent ADS 2013, Ansys-Ansoft Designer 8)—a method which is similarly known to be problematic (convergence and accuracy) when applied to oscillators with high Q resonators. The PN models depend on complex parameters and have no circuit focus and require special tools and efficient algorithms to evaluate the model parameters. The main drawbacks of this model is noise analysis mainly takes into account white noise sources, hence only PN with a $1/f^2$ characteristic, and it is therefore

TABLE 2. The relative strength and weakness of the three phase noise models for the characterization of oscillator circuits.

Model	Leeson	Lee and Hajimiri	Kaertner and Demir
Assumptions	LTIV	LTV	NLTV
Perturbing noise source	Constant white noise (KTB)	Cyclostationary $1/f^k$ for any $k \varepsilon N$	Modulated $1/f^k$ for any $k \varepsilon N$
Accuracy	Reasonable	Good	Exact
Simplicity	Simple	Moderate	Involved
Computer dependence	Independent (calculation by hand)	Computer to evaluate ISF	Computer dependent (no closed form solutions)
Predicts close-in phase noise	No	Good	Yes
Retained circuit parameters	Loaded Q-factor (Q_L), output power (P_s)	q_{max}	None

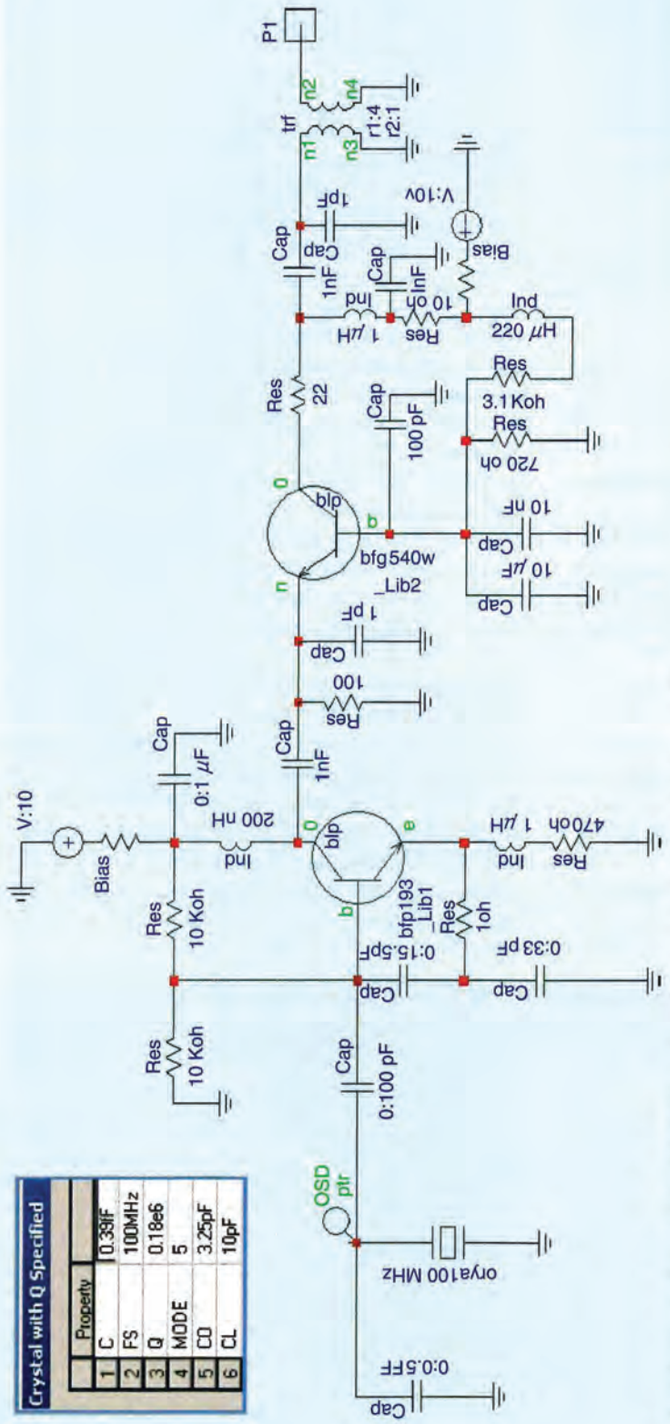

Figure 10. *A typical circuit schematic of a 100-MHz crystal oscillator with the grounded base amplifier.*

not straightforward to use their result in practical design and also numerical characterization of PN breaks down when extremely low PN crystal oscillators are considered. It mainly attempts to establish a foundation theory for the description of PN in nonlinear systems, which has been lacking earlier.

Ngoya et al. proposed PN model based on envelope transient simulation technique for arbitrary circuit topology [96]. The frequency conversion and modulation effects taking place in a free running oscillator as a result of noise perturbation are intimately linked within a single equation however PN model is not free from convergence problems for high Q resonator based oscillator circuits.

Multiple Threshold Crossing Noise Model

The noise models (LTIV, LTV and NLTV) explain the noise dynamics of LC resonator based harmonic oscillators. The LTIV, LTV, and NLTV models (all are frequency based) are good for resonant based (like LC, crystal) but not suitable for relaxation and ring oscillator circuits. In particular relaxation oscillator has noise jump/spikes (chaos/bifurcation) due to regeneration during transition, which cannot be easily modeled by frequency based methods. The poor PN performance of time/waveform based oscillators (like relaxation, ring, and multivibrator) limits the figure of merit (FOM) in RF systems as compared to harmonic oscillator (LC tank oscillator). There is a need to improve the PN performance of single energy storage reactive element (capacitor) oscillator such as RC oscillator (like relaxation and ring oscillators) for taking the advantage of integrated solution using existing MMIC technologies. The noise model based on threshold crossing is ideal for time/waveform based oscillator (like relaxation and ring).

Conclusion on Phase Noise Models (Harmonic Oscillators)

Table 2 describes the relative strength and weakness of the three PN

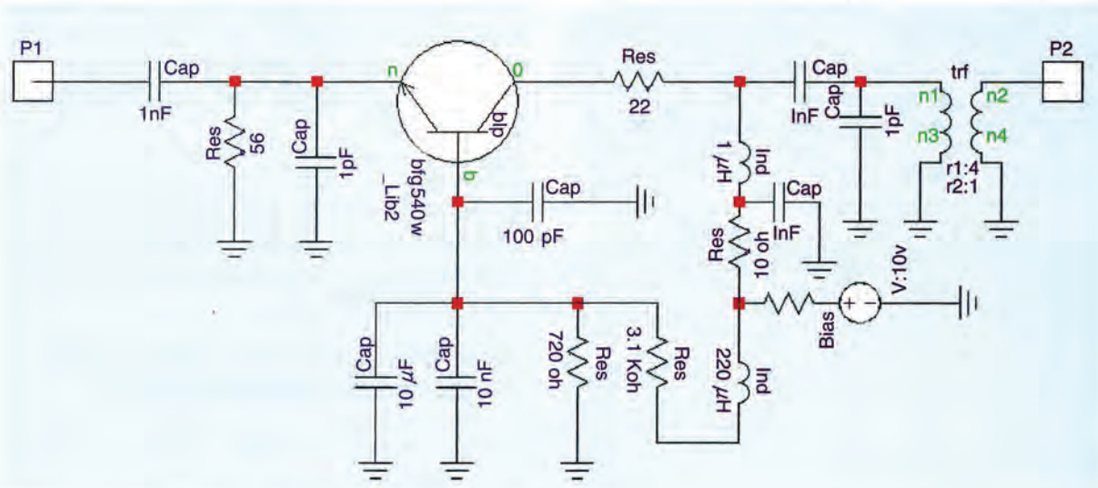

Figure 11. *A typical circuit of a low noise grounded base amplifier.*

models discussed above for the characterization of oscillator circuits.

All the three models discussed above are shown in Table 2 for harmonic oscillators, and one can argue the superiority of any of the three models based on accuracy, reliability, simulation time, and convergence for a given oscillator circuit topology.

In the noise model for nonharmonic oscillator circuits (proposed by A. Abidi, A. Hajimiri, B. Razavi, R. Navid, T. Lee, R. Dutton, and B. Leung) such as relaxation and ring oscillator circuits, Leung highlighted the inadequacy of traditional first passage time (FPT) model and the need for the last passage time (LPT) model in representing the threshold crossing behavior of time/waveform based oscillator. The noise model discusses the timing jitter based on the LPT model. Leung's noise model is based on multiple thresholds crossing concept, which considers the impact caused by both noise and slew rate changing as transistors change between triode/saturation. It also develops a link between the last passage and FPT model and indicates when the difference between the two models becomes significant. Using multiple thresholds crossing concept, a new and more accurate way of handling such region change is developed. For a typical ring oscillator with an arbitrary voltage swing, core transistors in delay cells move between saturation and triode region, resulting timing jitter accumulated within a particular region. Leung's LPT model for

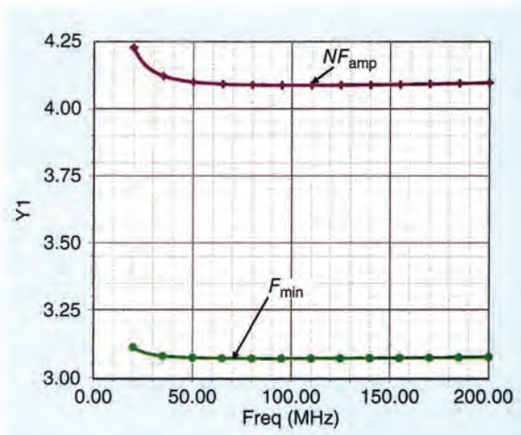

Figure 12. *A CAD simulated noise figure and F_{min} of the buffer amplifier shown in Figure 11 (the increase of the noise seen below 50 MHz is due to coupling capacitor).*

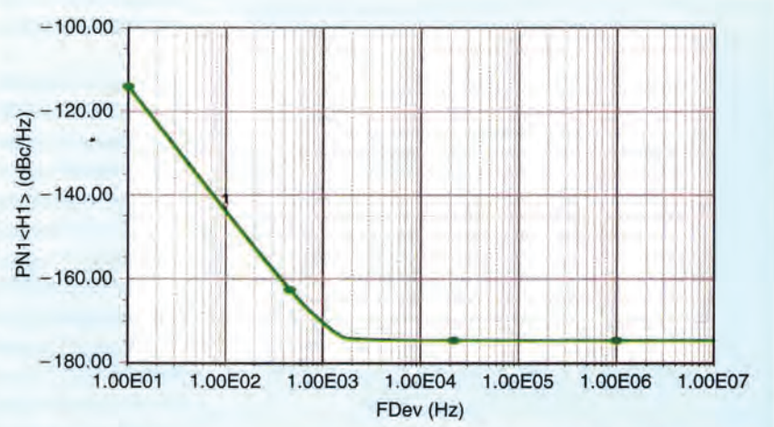

Figure 13. *A CAD simulated PN plot of a 100-MHz crystal oscillator circuit with buffer stage (Figure 11), −145 dBc/Hz at 100-Hz offset from the carrier frequency of 100 MHz.*

TABLE 3. Calculated noise figure and phase noise for 100-MHz crystal oscillator.

Oscillator Frequency	Calculated Large Signal Noise Figure	Phase Noise at 100-Hz Offset
100 MHz	7.72 dB	−146 dBc/Hz

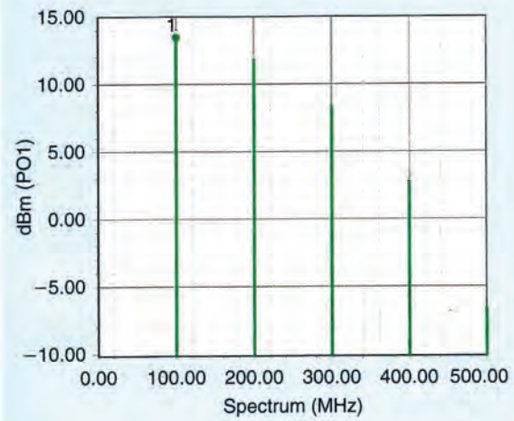

Figure 14. *A simulated power output plot of a 100-MHz crystal oscillator circuit with buffer stage (Figure 11).*

the threshold crossing offers more accurate description than the conventional FPT model when the noise/ramp ratio is not small.

Comparing the noise models discussed for harmonic (LC resonator type) and nonharmonic oscillator circuits (RC oscillator type), it is up to the designers to choose noise models for analyzing the autonomous circuits because none of the models allow closed form solution for PN-a unified solution needed for any typical oscillator circuit for a optimum FOM.

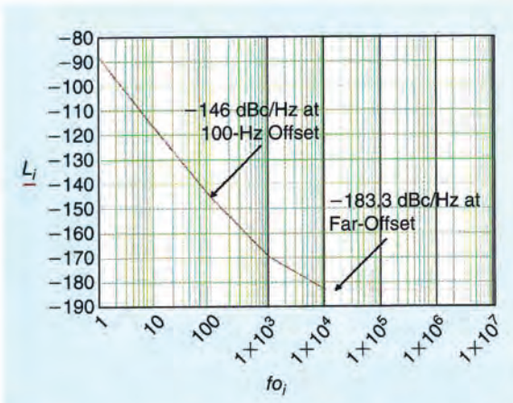

Figure 15. *A theoretically calculated PN plot for a 100-MHz crystal oscillator circuit shown in Figure (11) using PN model described in (8).*

Verification of Oscillator Phase Noise Model

Verification of 100-MHz Crystal Oscillator Using CAD Simulation Tool (Ansoft Designer from Ansys)

Figures 10–14 show the typical schematic of simplified Colpitts 100-MHz crystal oscillator circuit, grounded base buffer circuit, noise figure plots, PN plots, and output power for comparative analysis with theoretical and experimental treatment for the validation of PN analysis.

Verification of 100-MHz Crystal Oscillator Using Analytical Theoretical Model

The theoretical calculated parameters of 100-MHz crystal oscillator circuit shown in Figure 10 using PN model given in (8) is given in "Mathcad Analysis for 100-MHz Oscillator Circuit":

$$\text{Noise Fcator}(F) = 1 + \frac{Y_{21}^{+} C_2 C_c}{(C_1 + C_2) C_1} \times \left[r_b + \frac{1}{2r_e} \left(r_b + \frac{(C_1 + C_2) C_1}{Y_{21}^{+} C_2 C_c} \right)^2 \left(\frac{1}{\beta^{+}} + \frac{f^2}{f_T^2} \right) + \frac{r_e}{2} \right]. \quad (11)$$

Table 3 shows the calculated Noise Figure and PN for 100-MHz crystal oscillator using (11) and (8) for unloaded $Q = 200{,}000$ [4].

Figure 15 shows the theoretically calculated PN plot for 100-MHz crystal oscillator circuit shown in Figure 10 using PN model described in (8).

Verification of 100-MHz Crystal Oscillator Using Phase Noise Measurement Equipment

For validation of the CAD simulated and theoretical PN model described in Figures 13 and 15, 100-MHz crystal oscillator circuit (LNXO 100) was built and tested on different PN measurement equipment (Agilent E5052B, R&S FSUP, Holzworth, Noise XT, and Anapico APPH6000-IS) commercially available on the market.

Verification of 100-MHz Crystal Oscillator Using Agilent 5052B PN Measurement Equipment

The feature of cross-correlation techniques in Agilent E5052B satisfies the established criteria without additional references nor calibration of the device under test (DUT) on exact frequency. Figures 16 and 17 show the picture of Agilent E5052B equipment and measured PN plot of 100-MHz crystal oscillator circuit (LNXO 100) for the purpose of the verification of measurement uncertainty. The measured PN at 100 Hz offset is −143 dBc/Hz for LNXO 100 (100-MHz carrier frequency); this shows the capability of close-in measurement. The main concern is the dynamic range and noise floor of the equipment, measured at large offsets form the carrier, the far offset noise floor is −174 dBc/Hz

Mathcad Analysis for 100-MHz Oscillator Circuit

After defining all the values the phase noise can be correctly predicted

$C1 := 15.6\ pF$ $KT := 4.143 \cdot 10^{-21} \cdot J$ $qcharge := 1.602 \cdot 10^{-19} \cdot coul$ $y11 := (0.000884 - 0.0000158j) \cdot mho$

$C2 := 12.5\ pF$ $R := 0.2 \cdot \Omega$

$V_{cc} := 10$ $L := 1600 \cdot 10^{-9} \cdot henry$ $kf := 1 \cdot 10^{-10}$ $Ic := 28 \cdot mA$ $y21 := (-0.0105 - 0.00084j) \cdot mho$

$i := 0...7$ $p := 1.45$ $q := 1.05$ $Ib := 220 \cdot \mu A$ $Q_{mac} := 377$ $af := 2$ $Q := 200000$

$fc := 100 \cdot MHz$ $wc := 2\pi \cdot fc$ $nfdB := 7.7$

$fo_i := 10^i \cdot Hz$ $wo_i := 2 \cdot \pi \cdot fo_i$ $P_{out}dB := 14$

$$y := \frac{C1}{C2} \qquad B1_i := (wo_i)^2 \cdot L^2 \cdot V_{cc}^2$$

$$kconstant := \frac{KT \cdot R}{wc^2 \cdot C2^2} \qquad b := \frac{|y21|\cdot y^p}{|y11|} \qquad gm := |y21| \cdot y^q \qquad k0_i := \frac{kconstant}{B1_i}$$

$$k1constant_i := qcharge \cdot Ic \cdot gm^2 + \frac{kf \cdot Ib^{af} \cdot gm^2}{wo_i} \qquad t2_i := k0_i \cdot \frac{(1+y)^2}{y^2}$$

$$k1_i := \frac{k1constant_i}{wc^2 \cdot B1_i} \qquad k3_i := wc^2 \cdot gm^2 \qquad k2_i := wc^4 \cdot b^2$$

$$k_i := \frac{k3_i}{k2_i \cdot C2^2} \qquad t1_i := \left[\left(\frac{b^2}{gm^3} \right)^2 \cdot \frac{(k_i)^3 \cdot k1_i \cdot (wc)^2}{(y^2 + k_i)} \right] \cdot \frac{(1+y)^2}{y^2}$$

$$1_i := t1_i + t2_i$$

$$m_i = 10 \cdot \log\left[1_i \cdot (kg^{-2} \cdot m^{-4} \cdot s^5 \cdot A^2) \cdot \frac{Q_{mac}^2}{Q^2} \right]$$

$$L_i := \text{if}[m_i < (-(177 + P_{out}dB - nfdB)), (-(177 + P_{out}dB - nfdB)), m_i]$$

m_i	fo_i	L_i
−88.035	$1 \cdot s^{-1}$	−88.035
−117.814	$10 \cdot s^{-1}$	−117.814
−146.064	$100 \cdot s^{-1}$	−146.064
−169.714	$1 \cdot 10^3 \cdot s^{-1}$	−169.174
−190.327	$1 \cdot 10^4 \cdot s^{-1}$	−183.3
−210.394	$1 \cdot 10^5 \cdot s^{-1}$	−183.3
−230.4	$1 \cdot 10^6 \cdot s^{-1}$	−183.3
−250.401	$1 \cdot 10^7 \cdot s^{-1}$	−183.3

at offsets greater than 100 KHz. The theoretical expectations were closer to −184 dBc/Hz at 10 KHz offsets and beyond for 14 dBm output power with 7.72 dBm noise figure as shown in Table 3. The other problem is that the mixer and the post amplifier can easily get into compression which raises the noise floor.

Experimental Verification of 100-MHz Crystal Oscillator using Rohde & Schwarz (FSUP 26)

The feature of cross-correlation techniques in R&S (FSUP 26) satisfies the established criteria and neither requires additional references nor calibration of the DUT on exact frequency. Figures 18 and 19 show the picture of R&S (FSUP 26) equipment and measured PN plot *of* 100 MHz crystal oscillator for the purpose of the

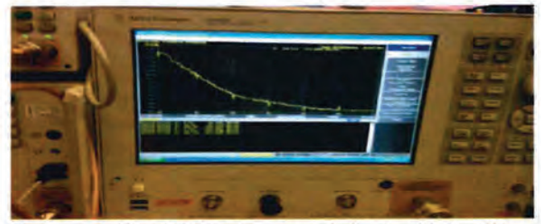

Figure 16. *The E5052B (courtesy: Agilent) with the PN plot of 100-MHz crystal oscillator circuit for the purpose of the verification of measurement uncertainty.*

verification of measurement uncertainty. The measured PN at 100 Hz offset is −140.74 dBc/Hz for LNXO 100 (100 MHz carrier frequency), and the far offset noise floor

Figure 17. *100 MHz crystal oscillator measured on agilent E5052B (Corr_4000).*

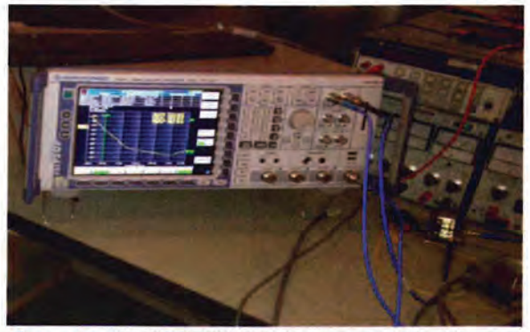

Figure 18. *The R&S FSUP 26 (courtesy: R&S) while taking measurement.*

is −183.42 dBc/Hz at offsets greater than 100 KHz. The theoretical expectations for close-in PN at 100 Hz offset is −146 dBc/Hz and noise floor closer to −184 dBc/Hz at 10 KHz offsets and beyond for 14 dBm output power.

Experimental Verification of 100-MHz Crystal Oscillator Using Anapico (APPH6000-IS)

The feature of cross-correlation techniques in APPH 6000 (Anapico) satisfies the established criteria but require two additional references at exact frequency. Figure 20 shows the screen-shot of Anapico PN measurement equipment, including the measured PN plot of 100-MHz crystal oscillator for the purpose of the verification of measurement uncertainty. The mesaured PN at 100 Hz-offset is −146 dBc/Hz for LNXO 100 (100-MHz carrier frequency), this shows the capability of close-in mesaurement. The instrument's specification calls for −184 dBc/Hz floor at offsets greater than 100 KHz. The theoretical expectations were closer to −184 dBc/Hz at 10-KHz offsets and beyond for 14 dBm output power. The main concern is the additional references at exact frequency of test oscillator circuits (DUT)

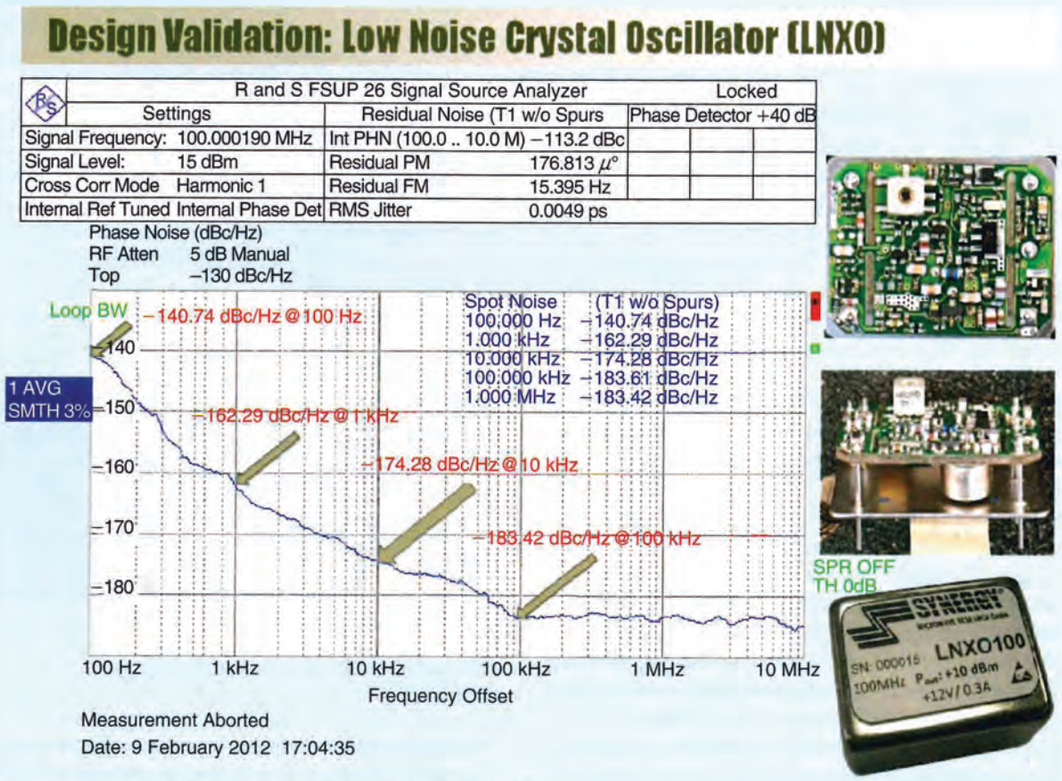

Figure 19. *A 100-MHz crystal oscillator measured on R&S FSUP.*

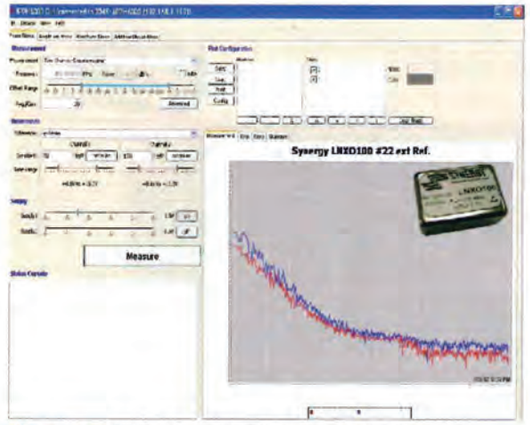

Figure 20. *PN plots and equipment setting (courtesy: Anapico APPH6000-IS) of a 100-MHz crystal oscillator measured on Anapico PN engine.*

Experimental Verification of 100-MHz Crystal Oscillator Using Holzworth

The feature of cross-correlation techniques in Holzworth system satisfies the established criteria; require two additional references at exact frequency. Figure 21

To overcome the limitation of LTV noise model, there have been several attempts to analyze the PN using NLTV techniques.

shows the picture of Holzworth PN measurement equipment, including the measured PN plot of 100-MHz crystal oscillator for the purpose of the verification of measurement uncertainty. The measured PN at 100 Hz offset is −147 dBc/Hz for LNXO 100 (100-MHz carrier frequency), this shows the capability of close-in mesaurement. The instrument's specification calls (conservatively) for −178 dBc/Hz floor at offsets greater than 100 KHz. The theoretical expectations were closer to −184 dBc/Hz at 10 KHz offsets and beyond for 14 dBm output power. The main concern is the additional references at exact frequency of test oscillator circuits (DUT).

Experimental Verification of 100-MHz Crystal Oscillator Using Noise XT (DCNTS)

The feature of cross-correlation techniques in Noise XT satisfies the established criteria; require two

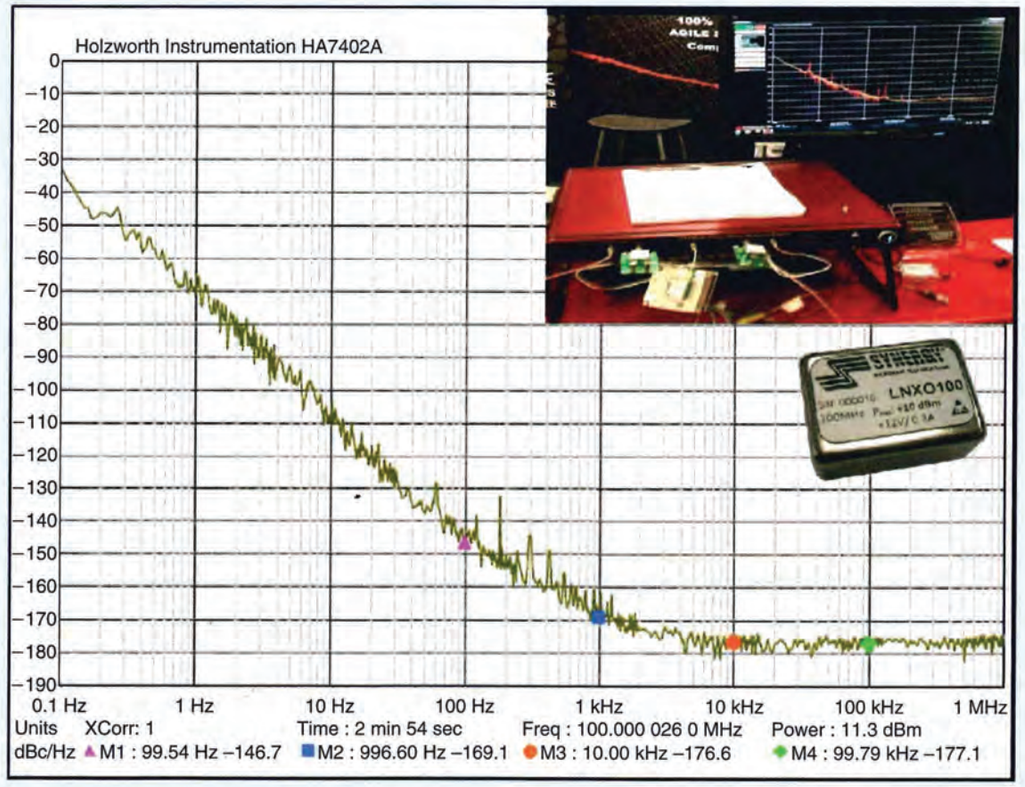

Figure 21. *PN plots and equipment setting (courtesy: Holzworth) of a 100-MHz crystal oscillator measured on Holzworth PN engine.*

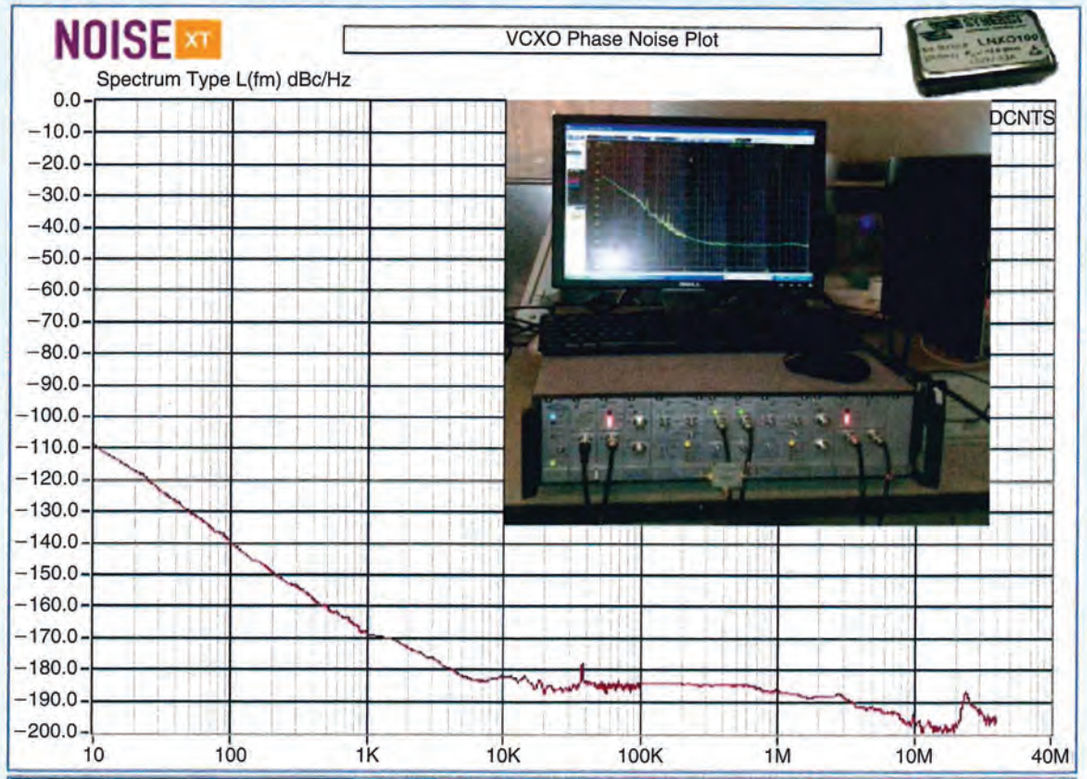

Figure 22. *LNXO 100 PN measurement using cross-correlation techniques (Noise XT DCNTS) LNXO 100 (100-MHz crystal oscillator) measured on noise XT DCNTS PN engine.*

TABLE 4. The theoretical and measured phase noise on different test equipment.

100-MHz OCXO *O/P* = 14 dBm, *NF* = 7 dB	Theoretical Model [1]	Agilent E5052B	R & S FSUP 26	Anapico APPH6000-IS	Holzworth HA7402-A	Noise XT DCNTS
At 100 Hz offset	−146 dBc/Hz	−143 dBc/Hz	−143 dBc/Hz	−141 dBc/Hz	−147 dBc/Hz	−140 dBc/Hz
At 1 kHz offset	−170 dBc/Hz	−167 dBc/Hz	−163 dBc/Hz	−170 dBc/Hz	−170 dBc/Hz	−170 dBc/Hz
At 10 kHz offset	−182 dBc/Hz	−173 dBc/Hz	−174 dBc/Hz	−172 dBc/Hz	−178 dBc/Hz	−181 dBc/Hz
At 100 KHz offset	−183 dBc/Hz	−174 dBc/Hz	−183 dBc/Hz	−181 dBc/Hz	−179 dBc/Hz	−183 dBc/Hz
At 1 MHz offset	−184 dBc/Hz	−174 dBc/Hz	−184 dBc/Hz	−182 dBc/Hz	−179 dBc/Hz	−186 dBc/Hz
At 10 MHz offset	−184 dBc/Hz	−174 dBc/Hz	−185 dBc/Hz	−188 dBc/Hz	−178 dBc/Hz	−196 dBc/Hz

additional references at exact frequency. Figure 22 show the picture of Noise XT (DCNTS) PN measurement equipment, including the measured PN plot of 100-MHz crystal oscillator for the purpose of the verification of measurement uncertainty. The mesaured PN at 100 Hz offset is −140 dBc/Hz for LNXO 100 (100-MHz carrier frequency), this shows the capability of close-in mesaurement. The instrument's specification calls (conservatively) for -195 dBc/Hz floor at offsets greater than 10 MHz. The theoretical expectations of -196 dBc/Hz noise floor closely met with this equipment for 14 dBm output power at 10-MHz offset. The main concern is the close-in PN which is 7 dB inferior as compared to Holzworth for identical correlations.

As shown in Figure 22, Noise XT Dual Core Noise Test Set (DCNTS) [28], [98] requires two references with similar performance as the DUT (the better the references' performance – the faster the test), the references must have voltage control (ability to change frequency with the change of the voltage on the control terminal), and be calibrated exactly on the frequency of DUT.

Phase Noise Measurement Evaluation and Uncertainties

The rigorous measurements were conducted on 100 MHz crystal oscillator using different PN Measurement Equipments (Agilent E5052B, R&S FSUP, Holzworth, Noise XT, and Anapico APPH6000-IS) available on the market. The PHENOM (OEwaves) is an ultrahigh performance automated PN test measurement system, utilizes microwave photonics techniques, and yields the spectral density of the PN of an RF or microwave signal source at any operating frequency in the specified bands. This homodyne-based system is unique in wide-frequency-band

Using multiple thresholds crossing concept, a new and more accurate way of handling such region change is developed.

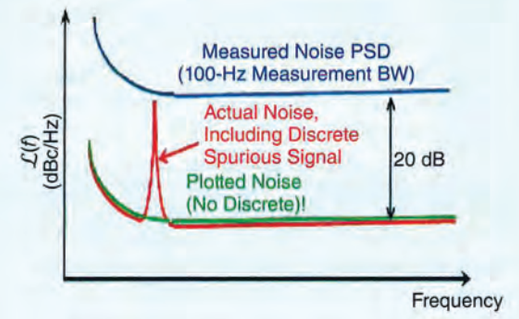

Figure 23. *An undetected discrete spurious signal.*

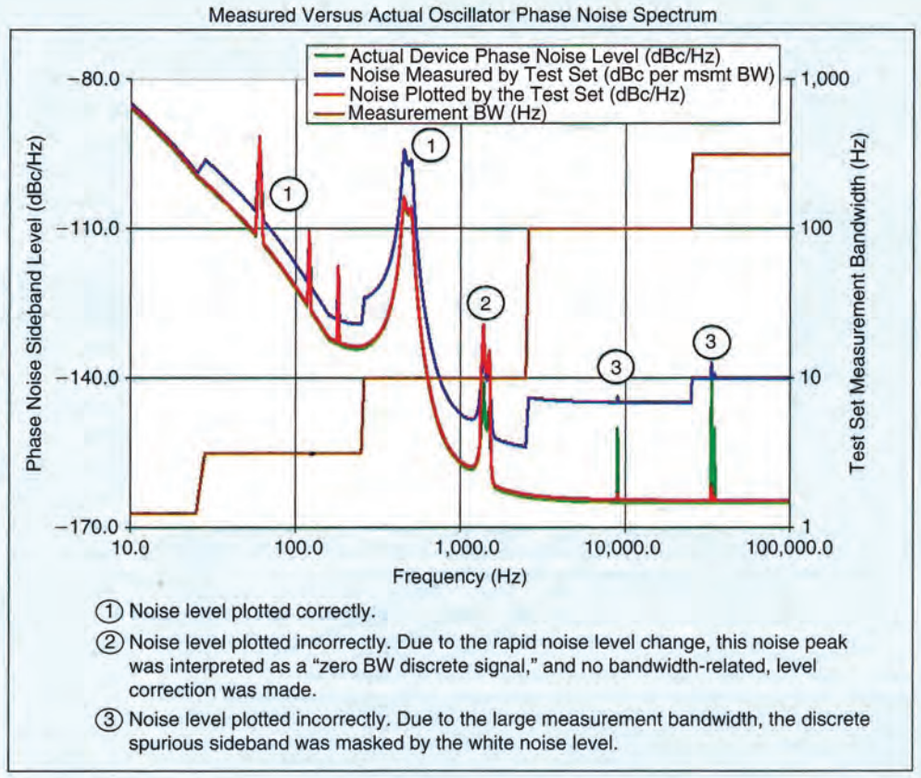

Figure 24. *The correct and erroneous display of PN data.*

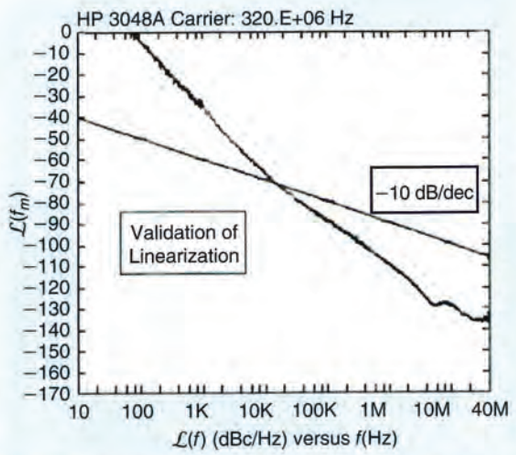

Figure 25. *Display of a typical PN measurement using the delay line principle. This method is applicable only where x _ sin(x). The measured values above the solid line violate this relationship and therefore are not valid.*

measurement without requiring another low-noise reference source or down-converter, as required in conventional heterodyne approaches. This equipment was not made available for the validation; nevertheless, the authors are keen to validate the measurement in the future using PHENOM for broader acceptance of the fact and myth linked with noise below the kT. Table 4 describes the theoretical and measured PN on different test equipment for comparative analysis of the measured data under similar test condition. Following is a set of measured results of 100-MHz crystal oscillators with different test equipments.

Phase Noise Measurement Issues

There are important measurement issues that, if not well understood, can lead to erroneous results and interpretations [97]–[103]. They involve measurement bandwidth masking of, and accurate distinction between, true discrete spurious signals and narrowband noise peaks (typically encountered under vibration). Although the PN data displayed by PN equipment is usually normalized to 1 Hz measurement bandwidth, most automated PN measurement equipment actually measures the PN in measurement bandwidths that increase with increasing carrier offset frequency. This is done for two reasons: 1) it results in shorter, overall measurement time and 2) at high carrier offset frequency (i.e., > 100 kHz), many measurement systems employ analog spectrum analyzers that are not capable of 1-Hz resolution. Noise measured in a 1-kHz bandwidth, for example, is 30 dB higher than that displayed in a 1 Hz bandwidth. That means that low level discrete spurious signals (and narrowband noise peaks typically encountered under vibration as a result of high Q mechanical resonances) may not be detected.

The second problem involves the software employed by the noise measurement system vendor used to discriminate between random noise and discrete spurious signals. Usually, when a reasonably sharp increase in noise level is detected, the system software assumes the increase marks the presence of a "zero bandwidth" discrete signal. It therefore (when displaying the PN on a 1 Hz bandwidth basis) applies a bandwidth correction factor to the random noise but does not make a correction to what was interpreted as a discrete signal. This results in an erroneous plot if/when the detected "discrete" is really a narrowband noise peak. Figures 23 and 24 attempt to depict the various situations that can result from these issues as described above.

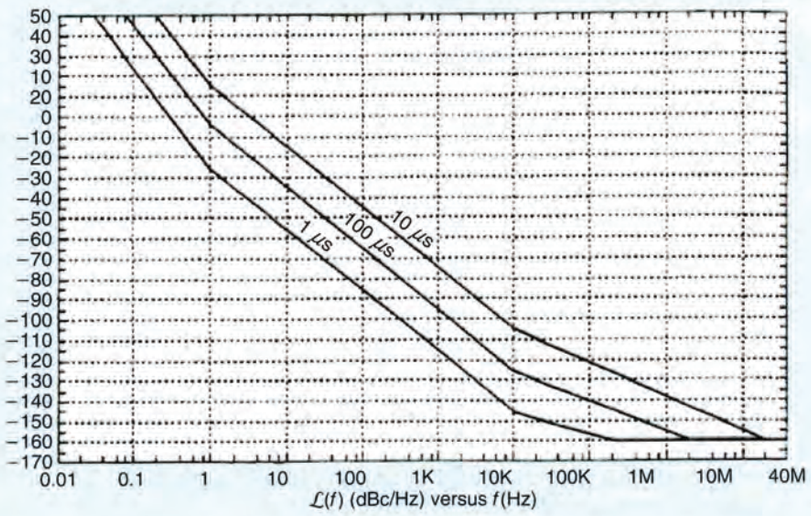

Figure 26. *Dynamic range as a function of cable delay. A delay line of 1 ms is ideal for microwave frequencies.*

Applying the Cross-Correlation

The old systems have an FFT analyzer for close-in calculations and are slower in speed. Modern equipments use noise-correlation method. The reason why the cross-correlation method became popular is that most oscillators have an output typically between 0 and 15 dBm and what's even more important is that only one single source is required. The method with a delay line, in reality requires a variable delay line to provide correct PN numbers as a function of offset. This is important and is shown in [4, pp. 148–153 Fig 7.25 and 7.26] and Figures 25 and 26 for a quick reference.

The feature of cross-correlation techniques in Holzworth system satisfies the established criteria.

Advantages of the Noise Correlation Technique

- Increased speed
- Requires less input power
- Single source set-up
- Can be extended from low frequencies like 1 MHz to 100 GHz

all depending upon the internal synthesizer.

Disadvantages of the Noise-Correlation Technique

- Different manufacturers have different isolation, so the available dynamic range is difficult to predict.
- These systems have a "sweet-spot," both R&S and Agilent start with an attenuator, not to

TABLE 5. Phase noise measurement related problems and possible remedy.

Serial No.	PN Measurement Related Issue	Possible Remedy
1	Reference noise compromise measurement	Obtain lower noise reference or use cross-correlation and two-independent references.
2	System noise compromise measurement	Use higher drive levels and/or higher drive level mixer.
3	Broadband okay, but *l/f* region too high	Look at a better reference or use carrier suppression or replace mixer.
4	System overall noise floor is too high	Change over to a cross-correlation topology.
5	Calibration has errors due to mixer/amplifier gain variations with offset frequency	Use an AM/PM calibration standard to measure the system at each offset frequency.
6	Residual detection of AM noise from Ref or DUT compromises measurement	See if a mixer with better balance will solve the problem or try to inject AM on the signal and adjust the phase balance (dc offset in the PLL loop) to minimize AM detection or switch to carrier suppression.
7	Injection locking is occurring	Improve the isolation between the sources and the mixer either by using an attenuator or an isolation amplifier. One may also need to look at power supplies or shielding.
8	PLL bandwidth compensating for the phase noise close to the carrier	Reduce the PLL gain or switch to the delay line discriminator approach or measure the amount of attenuation and compensate. This can be done using an AM/PM calibration standard.
9	PLL does not seem to be locking	Do you have the right tuning voltage for your PLL output matched to the tuning range of your source? Does the source tune far enough to match the frequency of the other source? An external bias to the tune might be necessary to get the source close to the desired operating frequency.
10	PLL still does not seem to work	Frequency-divide the sources to a much lower frequency. Since the phase excursion also is divided, much less PLL gain is required and, hence, the PM bias is much less.
11	The final plot has large excursions between the peaks and valleys	If you do not have a fairly fine line through the noise sections of the plot, the number of averages needs to be increased. See Table 1 for details.
12	Line harmonics are too high or causing excess measurement noise	Make sure all of the equipment is on the same side of the ac line. Look at using line filters, conditioners, or batteries. Consider using an inside/outside dc block. Move the measurement system away from high ac current sources and transformers.
13	Dynamic range limitation	It is possible to insert a notch filter between the test object and the analyzing receiver (or spectrum analyzer). This way, the carrier can be suppressed while the sideband noise is not much affected.

The reason why the cross-correlation method became popular is that most oscillators have an output typically between 0 and 15 dBm and what's even more important is that only one single source is required.

overload the two channels; 1 dB difference in input level can result in quite different measured numbers. These "sweet-spots" are different for each machine.

- The harmonic contents of the oscillator can cause an erroneous measurement [8], that's why a switchable-low-pass filter like the R&S (FSUP) or its equivalent should be used.
- Frequencies below 200 MHz, systems such as Anapico or Holzworth using 2 crystal oscillators instead of a synthesizer must be used. There is no synthesizer good enough for this measurement. Example: Synergy LNXO100 crystal oscillator measures about −142 dBc/Hz, 100 Hz after carrier, limited by the synthesizer of the FSUP and −147 dBc/Hz with the Holzworth system. Agilent results are similar to the R&S FSUP, just faster.
- At frequencies like 1 MHz off the carrier, these systems gave different results. The R&S FSUP, taking advantage of the "sweet-spot," measures −183 dBc, Agilent indicates −175 dBc/Hz and Holzworth measures −179 dBc/Hz.

We have not researched the "sweet-spots" for Agilent and Holzworth, but we have seen publications for both Agilent and Holzworth showing −190 dBc/Hz far off the carrier. These were selected crystal oscillators from either Wenzel or Pascall. Another problem is the physical length of the crystal oscillator connection cable to the measurement system. If the length provides something like "quarter-wave-resonance," incorrect measurements are possible. The list of disadvantages is quite long and there is a certain ambiguity whether or not to trust these measurements or can they be repeated.

Remarks

Characterizing the PN of a system or component is not necessarily very easy. Many different approaches are possible, but the key is to find the best approach for the measurement requirements at hand.

A survey of some of the more common topologies along with some possible trouble spots helps one to review and keep in mind the advantages and limitations of each approach. Table 5 describes the quick summary that addresses PN measurement related problems and possible remedy [50].

Conclusion

The task was for the theoretical study of oscillator PN models and conducting rigorous PN measurement analysis using commercially available PN measurement equipment. The objective of this article is to study the claims made by PN equipment companies that claim to be measuring below the KT noise floor using cross-correlation techniques. If the PN measurement equipment in use, after many correlations gives a better number which one may like to see, it violates the laws of physics as we understand them and if it gives a worse number, then either the correlations settings need to be corrected or the dynamic range of the equipment is insufficient. We realize that this treatment is exhaustive, but it was necessary to explain how things fall in place. At 20-dBm output, the output amplifier certainly has a higher noise figure, as it is driven with more power and there is no improvement possible. There is an optimum condition and some of the measurements showing −190 dBc/Hz doesn't seem to match the theoretical calculations. The correlation allows us to look below kT (where k is Boltzmann constant, T is temperature in Kelvin) but the usefulness of the noise contribution below KT is questionable and depends on applications. For better understanding, prototype of low noise ovenized controlled crystal oscillator (OCXO) was developed that measure typically −147 dBc/Hz at 100 Hz offset for 100-MHz OCXO and exhibit −185 dBc/Hz noise floor at far offset (10-MHz offset) with 14 dBm output power. The challenging exercise was to measure −195 dBc/Hz at far offset for output power of 20 dBm and the measured data should be reliable and repeatable. There are many areas in which design engineers can be tricked into false readings or frustrated with the process of trying to achieve a good measurement (below kT).

References

[1] D. B. Leeson, "A simple model of feedback oscillator noise spectrum," *Proc. IEEE*, vol. 54, no. 2, pp. 329–332, 1966.

[2] U. L. Rohde, A. K. Poddar, and R. Rebel, "Integrated low noise microwave wideband push-push VCO," U.S. Patent 7 088 189, Aug. 8, 2006

[3] K. Hosoya, S. Tanaka, Y. Amamiya, T. Niwa, H. Shimawaki, and K. Honjo, "A low phase-noise 38-GHz HBT MMIC oscillator utilizing a (l/4±d) open stubs resonator," in *Proc. Asia Pacific Microwave Conf.*, Singapore, 1999, pp. 64–67.

[4] U. L. Rohde, A. K. Poddar, and G. Boeck, *Modern Microwave Oscillators for Wireless Applications: Theory and Optimization*. Hoboken, NJ: Wiley, 2005.

[5] A. P. S. (Paul) Khanna, "Microwave oscillators: The state of the technology," *Microwave J.*, vol. 4, pp. 22–42, Apr. 2006.

[6] J. C. Nallatamby, M. Prigent, M. Camiade, and J. Obregon, "Phase noise in oscillators–Leeson formula revisited," *IEEE Trans. Microwave Theory Tech.*, vol. 51, no. 4, pp. 1386–1394, Apr. 2003.

[7] A. Suárez, S. Sancho, S. Ver Hoeye, and J. Portilla, "Analytical comparison between time- and frequency-domain techniques for phase-noise analysis," *IEEE Trans. Microwave Theory Tech.*, vol. 50, no. 10, pp. 2353–2361, Oct. 2002.

[8] S. Ver Hoeye, A. Suárez, and J. Portilla, "Techniques for oscillator nonlinear optimization and phase-noise analysis using commercial harmonic-balance software," in *IEEE MTT-S Dig.*, 2000, pp. 95–98.

[9] V. Rizzoli, F. Mastri, and D. Masotti, "General noise analysis of nonlinear microwave circuits by the piecewise harmonic balance technique," *IEEE Trans. Microwave Theory Tech.*, vol. 42, no. 5, pp. 807–819, May 1994.

[10] S. Sancho, A. Suárez, J. Domínguez, and F. Ramírez, "Analysis of near-carrier phase-noise spectrum in free-running oscillators in the presence of white and colored noise sources," *IEEE Trans. Microwave Theory Tech.*, vol. 58, no. 3, pp. 587–601, Mar. 2010.

[11] S. Romisch and R. Lutwak, "Low-power, 4.6-GHz, stable oscillator for CSAC," in *Proc. IEEE Int. Frequency Control Symp. Expo.*, Miami, FL, 2006, pp. 448–451.

[12] A. K. Poddar, S. K. Koul, and B. Bhat, "Millimeter wave evanescent mode gunn diode oscillator in suspended stripline configuration," in *Proc. IR & MM Wave, 22nd Int. Conf.*, July 1997, pp. 265–266.

[13] M.-S. Yim and K. K. O, "Switched resonators and their applications in a dual band monolithic CMOS LC tuned VCO," *IEEE Trans. Microwave Theory Tech.*, vol. 54, no. 1, pp. 74–81, Jan. 2006.

[14] N. Nomura, M. Itagaki, and Y. Aoyagi, "Small packaged VCSO for 10 Gbit Ethernet application," in *Proc. IEEE Int. Frequency Control Symp. Exposition*, 2004, pp. 418–421.

[15] J.-H. Lin and Y.-H. Kao, "A low phase noise voltage controlled SAW oscillator with surface transverse wave resonator for SONET applications," *IEEE Trans. Microwave Theory Tech*, vol. 55, no. 1, pp. 60–65, Jan. 2007.

[16] J. S. Hong and M. J. Lancaster, "Aperture-coupled microstrip open-loop resonators and their applications to the design of novel microstrip bandpass filters," *IEEE Trans. Microwave Theory Tech.*, vol. 47, no. 9, pp. 1848–1855, Sept. 1999.

[17] J.-S. Hong and M. J. Lancaster, "Coupling of microstrip square open-loop resonators for cross-coupled planar microwave," *IEEE Trans. Microwave Theory Tech.*, vol. 44, no. 12, pp. 2099–2109, Dec. 1996.

[18] S. Sun and L. Zhu, "Guided-wave characteristics of periodically nonuniform coupled microstrip lines-even and odd modes," *IEEE Trans. Microwave Theory Tech.*, vol. 53, no. 4, pp. 1221–1227, Apr. 2005.

[19] U. L. Rohde and A. K. Poddar, "Tunable frequency, low phase noise and low thermal drift oscillator," U.S. Patent 7 196 591, Mar. 1, 2007.

[20] U. L. Rohde and A. K. Poddar, "Wideband voltage controlled oscillators employing evanescent mode coupled resonators," U.S. Patent 71 803 812, Feb. 20, 2007.

[21] U. L. Rohde, "A new efficient method of designing low noise microwave oscillators," Dr.-Ing. (Ph.D.) dissertation, Faculty IV, Elect. Eng. Comp. Sci., Tech. Univ., Berlin, Germany, 2004.

[22] U. L. Rohde, A. K. Poddar, J. Schoepf, R. Rebel, and P. Patel, "Low noise low cost wideband N-push VCO," in *IEEE MTT-S Int. Microwave Symp. Dig.*, 2005, pp. 1171–1174.

[23] A. K. Poddar, "A novel approach for designing integrated ultra low noise microwave wideband voltage-controlled oscillators," Dr.-Ing. (Ph.D.) Dissertation, Faculty IV, Elect. Eng. Comp. Sci., Tech. Univ., Berlin, Germany, 2004.

[24] U. L. Rohde, A. K. Poddar, and R. Rebel, "Ultra low noise low cost octave-band hybrid-tuned VCO," in *Proc. Electrical Computer Engineering, Canadian Conf.*, Saskatoon, SK, Canada, 2005, pp. 831–834.

[25] U. L. Rohde and A. K. Poddar, "Ultra low noise low cost multi octave band VCO," in *Proc. IEEE Sarnoff Symp.*, Princeton, NJ, Apr. 2005, pp. 5–8.

[26] A. K. Poddar and K. N. Pandey, "Microwave switch using MEMS-technology," in *Proc. 8th IEEE Int. Symp. High Performance Electron Device for Microwave Optoelectronic Applications*, Nov. 2000, pp. 134–139.

[27] U. L. Rohde and A. K. Poddar, "Configurable ultra low ultra wideband power efficient VCOs," in *Proc. 11th European Wireless, Conf.*, Nicosia, Cyprus, Apr. 10–13, 2005. pp. 1–7.

[28] U. L. Rohde, K. J. Schoepf, and A. K. Poddar, "Low-noise VCOs conquer wide bands," *Microwave & RF*, vol. 8, pp. 98–106, June 2004.

[29] U. L. Rohde and A. K. Poddar, "Configurable adaptive ultra low noise wideband VCOs," in *Proc. IEEE Int. Conf. Ultra-Wideband*, Switzerland, Sept. 5–8, 2005, pp. 452–457.

[30] U. L. Rohde and A. K. Poddar, "Reconfigurable wideband VCOs," in *Proc. IEEE 16th Int. Symp. Personal, Indoor Mobile Radio Communications*, Berlin, Germany, Sept. 11–14, 2005, pp. 1250–1253.

[31] U. L. Rohde and A. K. Poddar, "Ultrawideband RF signal source," in *Proc. IEEE 2nd Int. Symp. Wireless Communication Systems*, Siena, Italy, Sept. 2005, pp. 255–258.

[32] W. To-Po, Z.-M. Tsai, K.-J. Sun, and H. Wang, "Phase-noise reduction of X-band push-push oscillator with second-harmonic self-injection techniques," *IEEE Trans. Microwave Theory Tech.*, vol. 55, no. 1, pp. 66–77, Jan. 2007.

[33] K. Hoffmann and Z. Skvor, "Active resonator," in *Proc. EURO-CON, Trends in Communications, Int. Conf.*, Bratislava, Slovakia, 2001, vol. 1, pp. 164–166.

[34] W. P. Robins, *Phase Noise in Signal Sources*. London: IEE Telecommunications Series 9, 1982.

[35] T. H. Lee and A. Hajimiri, "Oscillatator phase-noise: A tutorial," *IEEE J. Solid-State Circuits*, vol. 35, no. 3, pp. 326–336, Mar. 2000.

[36] A. Hajimiri and T. H. Lee, "A general theory of phase noise in electrical oscillators," *IEEE J. Solid-State Circuits*, vol. 33, no. 2, pp. 179–194, Feb. 1998.

[37] D. B. Sullivan, "Characterization of clocks and oscillators," National Bureau of Standards Tech. Note 1337, 1990.

[38] A. Demir, A. Mehrotra, and J. Roychowdhury, "Phase noise in oscillators: A unifying theory and numerical methods for characterization," *IEEE Trans. Circuits Syst. I, Fundam. Theory Applicat.*, vol. 47, no. 5, pp. 655–674, May 2000.

[39] M. Nick, "New Q-enhanced planar resonators for low phase-noise radio frequency oscillators," Ph.D. dissertation, Dept. Electrical Eng., Michigan Univ., Ann Arbor, MI, 2011

[40] V. Rizzoli, A. Neri, A. Costanzo, and F. Mastri, "Modern harmonic-balance techniques for oscillator analysis and optimization," in *RF and Microwave Oscillator Design*, M. Odyniec, Ed. Boston, MA: Artech House, 2002, ch. 5.

[41] B. Razavi, "A study of phase-noise in CMOS oscillators," *IEEE J. Solid-State Circuits*, vol. 31, no. 3, pp. 331–343, Mar. 1996.

[42] A. Demir, A. Mehrotra, and J. Roychowdhury, "Phase noise in oscillators: A unifying theory and numerical methods for characterization," *IEEE Trans. Circuits Systems I, Fundam. Theory Applicat.*, vol. 47, no. 5, pp. 655–674, May 2000.

[43] A. Hajimiri and T. H. Lee, "Design issues in CMOS differential LC oscillators," *IEEE J. Solid-State Circuits*, vol. 34, no. 5, pp. 717–724, May 1999.

[44] A. Hajimiri and T. H. Lee, *The Design Of Low Noise Oscillators*. Boston, MA: Kluwer Academic, 1999

[45] A. Hajimiri and T. H. Lee, "Oscillator phase noise: A tutorial," *IEEE J. Solid-State Circuits*, vol. 35, no. 3, pp. 326–336, Mar. 2000.

[46] F. X. Kaertner, "Analysis of white and _übNoise in oscillators," *Int J. Circuit Theory Applicat.*, vol. 18, pp. 485–519, Oct. 1990.

[47] A. Demir, "Phase noise and timing jitter in oscillators with colored-noise sources," *IEEE Trans. Circuits Syst. I*, vol. 49, no. 12, pp. 1782–1791, Dec. 2002.

[48] G. J. Coram, "A simple 2-D oscillator to determine the correct decomposition of perturbations into amplitude and phase noise," *IEEE Trans. Circuits Syst. I*, vol. 48, no. 7, pp. 896–898, July 2001.

[49] (2012). Agilent phase noise measurement solution. [Online]. Available: www.home.agilent.com/agilent/application

[50] W. F. Walls, "Practical problems involving phase noise measurements," in *Proc. 33rd Annu. Precise Time Time Interval (P77'1) Meeting*, 2001, pp. 407–416.

[51] A. L. Lance, W. D. Seal, F. G. Mendozo, and N. W. Hudson, "Automating phase noise measurements in the frequency domain," in *Proc. 31st Annu. Symp. Frequency Control*, 1977, pp. 347–358.

[52] W. F. Walls, "Cross-correlation phase noise measurements," in *Proc. IEEE Frequency Control Symp.*, 1992, pp. 257–261.

[53] W. F. Walls, "Practical problems involving phase noise measurements," in *Proc. 33th Annu. Precise Time Interval Meeting*, 2001, pp. 407–416.

[54] F. L. Walls, A. J. D. Clements, C. M. Felton, M. A. Lombardi, and M. D. Vanek, "Extending the range and accuracy of phase noise measurements," in *Proc 42nd Annu. Symp. Frequency Control*, 1988, pp. 432–441.

[55] *Agilent E5052A Signal Source Analyzer 10 MHz to 7, 26.5, or 110 GHz—Datasheet*, Agilent Document 5989–0903EN, Santa Clara, CA, 2009, p. 12.
[56] *Frequency Extension for Phase Noise Measurements with FSUP26/50 and Option B60 (Cross-Correlation)*, Rohde & Schwarz Application Note 1EF56, Munich, Germany, 2007, p. 3.
[57] M. Jankovic, "Phase noise in microwave oscillators and amplifiers," Ph.D. dissertation, Dept. Elect., Comput. Energy Eng., Facul. Grad. Sch. Univ. Colorado, Boulder, Colorado, 2010.
[58] Hewlett Packard. (2010, Apr. 28). RF and microwave phase noise measurement seminar. [Online]. Available: http://www.hparchive.com/seminar_notes/HP_PN_seminar.pdf
[59] S. R. Kurz. (2010, May 11). WJ Tech note—Mixers as phase detectors. [Online]. Available: http://www.triquint.com/prodserv/tech_info/docs/WJ_classics/Mixers_phase_detectors.pdf
[60] Agilent Technologies. (2010, May 10). Phase noise characterization of microwave oscillators—Phase detector method—Product Note 11729B–1. [Online]. Available: http://tycho.usno.navy.mil/ptti/ptti2001/paper42.pdf
[61] Aeroflex. (2010, Apr. 28). Application Note #2—PN9000 automated phase noise measurement system. [Online]. Available: http://www.datasheetarchive.com/datasheetpdf/010/DSA00173368.html
[62] Hewlett Packard. (1989, Sept. 01). HP 3048A phase noise measurement system reference manual. [Online]. Available: http://cp.literature.agilent.com/litweb/pdf/03048–90002.pdf
[63] E. Rubiola and F. Vernotte. (2010, Feb. 27). The cross-spectrum experimental method. [Online]. Available: http://arxiv.org/,document arXiv: 1003.0113v1 [physics.ins-det]
[64] Hewlett Packard. (1990, June 01). HP 3048A phase noise measurement system operating manual. [online]. Available: http://cp.literature.agilent.com/litweb/pdf/03048–61004.pdf
[65] *HP 11848A Phase Noise Interface Service Manual*, 1st ed., Hewlett-Packard Company, Spokane, Washington, 1987.
[66] M. Sampietro, L. Fasoli, and G. Ferrari, "Spectrum analyzer with noise reduction by crosscorrelation technique on two channels," *Rev. Sci. Instrum.*, vol. 70, no. 5, pp. 2520–2525, May 1999.
[67] A. A. Abidi and R. G. Meyer, "Noise in relaxation oscillators," *IEEE J. Solid-State Circuits*, vol. SC–18, no. 6, pp. 794–802, Dec. 1983.
[68] B. W. Stuck, "Switching-time jitter statistics for bipolar transistor threshold crossing detectors," M.S. thesis, Dept. Elect. Eng., Massachusetts Inst. Technol., Cambridge, MA, 1969.
[69] A. Abidi. (1997, Nov.). How phase noise appears in oscillators. [Online]. Available: http://www.rfdh.com/ez/system/db/pds_tn/upload/271/phase_noise.pdf
[70] R. Navid, T. H. Lee, and R. W. Dutton, "Minimum achievable phase noise of RC oscillators," *IEEE J. Solid-State Circuits*, vol. 40, no. 3, pp. 630–637, Mar. 2005.
[71] L. DeVito, J. Newton, R. Croughwell, J. Bulzacchelli, and F. Benkley, "A 52 MHz and 155 MHz clock-recovery PLL," in *IEEE ISSCC Dig. Tech. Papers*, Feb. 1991, pp. 142–143.
[72] I. A. Young, J. K. Greason, and K. L. Wong, "APLL clock generator with 5 to 110 MHz of lock range for microprocessors," *IEEE J. Solid-State Circuits*, vol. 27, no. 11, pp. 1599–1607, Nov. 1992.
[73] A. Hajimiri, S. Limotyrakis, and T. H. Lee, "Jitter and phase noise in ring oscillators," *IEEE J. Solid-State Circuits*, vol. 34, no. 6, pp. 790–804, June 1999.
[74] R. Navid, T. H. Lee, and R. W. Dutton, "Lumped, inductorless oscillators: How far can they go?" in *Proc. IEEE Custom Integrated Circuits Conf.*, Sept. 2003, pp. 543–546.
[75] A. A. Abidi and R. G. Meyer, "Noise in relaxation oscillators," *IEEE J. Solid-State Circuits*, vol. 18, no. 12, pp. 794–802, Dec. 1988.
[76] B. Oksendal, *Stochastic Differential Equations*. Berlin, Heidelberg: Springer-Verlag, 1998.
[77] R. A. Silverman, *Topics in the Theory of Random Noise*, R. L. Stratonovich, Ed. New York: Gordon and Breach, 1963.
[78] R. Navid, T. H. Lee, and R. W. Dutton, "An analytical formulation of phase noise of signals with Gaussian distribution jitter," *IEEE Trans. Circuits Syst. II*, vol. 52, no. 3, pp. 149–153, Mar. 2005.
[79] B. Razavi, "A study of phase noise in CMOS oscillators," *IEEE J. Solid-State Circuits*, vol. 31, no. 3, pp. 331–343, Mar. 1996.
[80] J. G. Sneep and C. J. M. Verhoeven, "A new low-noise 100-MHz balanced relaxation oscillator," *IEEE J. Solid-State Circuits*, vol. 25, no. 6, pp. 692–698, June 1990.
[81] F. Herzel, M. Pierschel, P. Weger, and M. Tiebout, "Phase noise in a differential CMOS voltage-controlled oscillator for RF applications," *IEEE Trans. Circuits Syst. II, Analog Digital Signal Process.*, vol. CAS2–47, no. 1, pp. 11–15, Jan. 2000.
[82] Y. P. Tsividis, *Operation and Modeling of MOS Transistors*. New York: McGraw-Hill, 1999.
[83] J. G. Maneatis and M. A. Horowitz, "Precise delay generation using coupled oscillators," *IEEE J. Solid-State Circuits*, vol. 28, no. 12, pp. 1273–1282, Dec. 1993.
[84] H. Chang, X. Cao, U. K. Mishra, and R. A. York, "Phase noise in coupled oscillators: Theory and experiment," *IEEE Trans. Microwave Theory Tech.*, vol. MTT–45, no. 5, pp. 604–615, May 1997.
[85] R. Navid and R. W. Dutton, "The physical phenomena responsible for excess noise in short-channel MOS devices," in *Int. Conf. Simulation Semiconductor Processes Devices Dig. Tech. Papers*, Sept. 2002, pp. 75–78.
[86] B. H. Leung, "A novel model on phase noise of ring oscillator based on last passage time," *IEEE Trans. Circuits Syst. I, Reg. Papers*, vol. 51, no. 3, pp. 471–482, Mar. 2004.
[87] B. Leung, "A switching based phase noise model for CMOS ring oscillators based on multiple thresholds crossing," *IEEE Trans. Circuits Syst. I, Reg. Papers*, vol. 57, no. 11, pp. 2858–2869, Nov. 2010.
[88] B. Leung and D. Mcleish, "Phase noise of a class of ring oscillators having unsaturated outputs with focus on cycle to cycle correlation," *IEEE Trans. Circuits Syst. I, Reg. Papers*, vol. 56, no. 8, pp. 1689–1707, Aug. 2009.
[89] N. Lam and B. Leung, "Dynamic quadrant swapping scheme implemented in a post conversion block for I, Q, mismatch reduction in a DQPSK receiver," *IEEE J. Solid-State Circuits*, vol. 45, no. 2, pp. 322–337, Feb. 2012.
[90] B. Leung, "Comparison of phase noise models on a class of ring oscillators using low voltage swing fully differential delay cells," *Analog Integr. Circuits Signal Process.*, vol. 61, no. 2, pp. 129–147, Nov. 2009.
[91] Z. Shu, K. Lee, B. Leung, "A 2.4 GHz ring oscillator based CMOS frequency synthesizer with a fractional divider dual PLL architecture," *IEEE J. Solid-State Circuits*, vol. 39, pp. 452–463, Mar. 2004.
[92] B. Leung, "A novel model on phase noise in ring oscillator based on last passage time," *IEEE Trans. Circuits Syst. I, Reg. Papers*, vol. 51, pp. 471–482, Mar. 2004.
[93] B. Leung and D. Mcleish, "Investigation of phase noise of ring oscillators with time varying current and noise sources by time scaling thermal noise," *IEEE Trans. Circuits Syst. I, Reg. Papers*, vol. 51, pp. 1926–1939, Oct. 2004.
[94] M. Haidi and B. Leung, "PLL based frequency discriminator using the loop filter as an estimator," *IEEE Trans. Circuits Syst. II*, vol. 49, no. 11, pp. 721–727, Nov. 2002
[95] A. A. Abidi, "Phase noise and jitter in CMOS ring oscillators," *IEEE J. Solid-State Circuits*, vol. 41, no. 8, pp. 1803–1816, Aug. 2006.
[96] E. Ngoya, J. Rousset, and D. Argollo, "Rigrous RF and microwave oscillator phase noise calculation by envelope transient technique," in *IEEE Microwave Symp. Dig. MTT-S Int.*, 2000, vol. 1, pp. 91–94.
[97] M. M. Driscoll, "Modeling phase noise in multifunction subassemblies," *IEEE Trans. Ultrason. Ferroelectr. Freq. Control*, vol. 59, no. 3, pp. 373–381, Mar. 2012.
[98] *Noise XT*, DCNTS Manual. (2013). [Online]. Available: http:/www.noisext.com/pdf/noisext_DCNTS.pdf
[99] A. K. Poddar and U. L. Rohde, "Techniques minimize the phase noise in crystal oscillators," in *Proc. IEEE Int. Frequency Control Symp.*, May 2012, pp. 01–07.
[100] A. K. Poddar, "Expert tips, tricks and techniques," *Microwave J.*, vol. 7, p. 22, July 2012.
[101] A. K. Poddar and U. L. Rohde, "Latest technology, technological challenges, and market trends for frequency generating and timing devices," *IEEE Microwave Mag.*, vol. 13, pp. 120–134, Oct. 2012.
[102] D. Calbaza, C. Gupta, U. L. Rohde, and A. K. Poddar, "Harmonics induced uncertainty in phase noise measurements," in *IEEE MTT-S Int. Microwave Symp. Dig.*, June 2012, pp. 1–3.
[103] U. L. Rohde and A. K. Poddar, "Noise minimization techniques for voltage controlled crystal oscillator circuits," in *Proc. IEEE Radio Wireless Symp.*, San Diego, CA, Jan. 18–22, 2009, pp. 280–283.